

# QCD sum rule analysis of Heavy Quarkonium states in magnetized matter – effects of magnetic catalysis

Pallabi Parui,<sup>\*</sup> Sourodeep De,<sup>†</sup> Ankit Kumar,<sup>‡</sup> and Amruta Mishra<sup>§</sup>

*Department of Physics, Indian Institute of Technology, Delhi, New Delhi - 110016*

## Abstract

The in-medium masses of the  $1S$  and  $1P$  states of heavy quarkonia are investigated in the strongly magnetized (asymmetric) nuclear medium, using the QCD sum rule framework. These are calculated from the in-medium scalar and twist-2 gluon condensates, calculated within a chiral effective model. The gluon condensate is simulated through a scalar dilaton field  $\chi$  introduced in the model through a scale-invariance breaking logarithmic potential. The effects of magnetized Dirac sea contributions are incorporated in the present study through the baryonic tadpole diagrams. Treating the scalar fields as classical, the values of the dilaton field,  $\chi$  and the scalar fields (non-strange isoscalar,  $\sigma(\sim \langle \bar{u}u \rangle)$ , the strange isoscalar,  $\zeta(\sim \langle \bar{s}s \rangle)$  and nonstrange isovector,  $\delta(\sim (\langle \bar{u}u \rangle - \langle \bar{d}d \rangle))$ ) are obtained by solving the coupled equations of motion of these fields in the chiral effective model. The contribution of the Dirac sea is observed to lead to the magnetic catalysis effect, i.e, the rising values of the quark condensates, which are given in terms of the scalar fields, with increasing magnetic field. The in-medium masses of the charmonium and bottomonium ground states are observed to have appreciable modifications with magnetic field due to the Dirac sea contributions. In the presence of a magnetic field, there is also mixing between the longitudinal component of the vector meson and the pseudoscalar meson (PV mixing) in both quarkonia sectors, leading to rise (drop) of the masses of  $J/\Psi^{\parallel}(\eta_c)$  and  $\Upsilon^{\parallel}(1S)(\eta_b)$  states. The magnetic catalysis effect, along with the splittings between  $(J/\Psi^{\parallel} - \eta_c)$  and  $(\Upsilon(1S)^{\parallel} - \eta_b)$  quarkonia states due to the mixing effects, are observed to be large at high magnetic fields. These might show in the experimental observables, e.g., the dilepton spectra in non-central ultra-relativistic heavy ion collision experiments at RHIC and LHC, where the produced magnetic field is huge.

---

<sup>\*</sup>Electronic address: pallabiparui123@gmail.com

<sup>†</sup>Electronic address: sourodeepde2015@gmail.com

<sup>‡</sup>Electronic address: ankitchahal17795@gmail.com

<sup>§</sup>Electronic address: amruta@physics.iitd.ac.in

## I. INTRODUCTION

The study of the in-medium properties of hadrons is an important area of research in the physics of strongly interacting matter. The study of the heavy flavor hadrons [1] has attracted a lot of attention due to its relevance in the ultra-relativistic heavy ion collision experiments. Recently, heavy quarkonia ( $\bar{q}q; q = c, b$ ) under extreme conditions of matter, i.e., high density and/or high temperature, have been investigated extensively. The medium, created in the relativistic high energy collisions between heavy nuclei, affect the masses and decay widths of the particles, which can have further observable impacts, e.g., the production and propagation of the particles. In the non-central heavy ion collision experiments, strong magnetic fields are expected to be produced [2–5]. The magnetic fields produced, have been estimated to be huge in RHIC, BNL and in LHC, CERN [6]. However, the time evolution of the magnetic field produced in such experiments requires the detailed knowledge of the electrical conductivity of the medium and careful treatment of the solutions of magneto-hydrodynamic equations [6] and is still an open question. The study of the effects of strong magnetic fields on the in-medium properties of hadrons has initiated a new area of research in the heavy ion physics.

The heavy quarkonium (charmonium and bottomonium) states have been investigated in the literature using the potential models [7–9], the QCD sum rule approach [10–14], coupled channel approach [16], the quark-meson coupling model [17, 18], a chiral effective model [19, 20, 31], and a field theoretic model for composite hadrons [32, 33]. In the present work, we study the masses of the S-wave (Vector,  $J/\Psi$ , Pseudoscalar,  $\eta_c$ ) and P-wave (scalar,  $\chi_{c0}$ , axial vector  $\chi_{c1}$ ) charmonium and and S-wave (Vector,  $\Upsilon(1S)$ , Pseudoscalar,  $\eta_b$ ) and P-wave (scalar,  $\chi_{b0}$ , axial vector  $\chi_{b1}$ ) bottomonium ground states, within the magnetized, isospin asymmetric nuclear medium using the formalism of QCD sum rule by incorporating the effect of Dirac sea in the presence of an external magnetic field.

The S-wave and P-wave charmonium and bottomonium ground states have been studied in magnetized nuclear matter, without the effect from Dirac sea [14, 15, 34] by the sum rule formalism. The medium effects are incorporated through the QCD gluon condensates [35], up to dimension 4, in terms of the medium modifications of scalar fields within a chiral  $SU(3)$  model based on the non-linear realization of chiral  $SU(3)_L \times SU(3)_R$  symmetry. In our present study, we have considered the effects of magnetic field on the Dirac sea

polarizations in addition to the Landau levels contributions of protons in the magnetized nuclear medium, within the chiral  $SU(3)$  model. The effects of magnetic field on the QCD vacuum condensates are seen to be important through the magnetic field modified Dirac sea polarizations. The light quark condensates tend to rise with magnetic field, an effect called magnetic catalysis [21–24]. In the literature, this effect has been studied in a large extent on the quark matter sector using the Nambu-Jona-Lasinio (NJL) model [25–27]. In [28], the effects of magnetic catalysis have been studied on the nuclear matter within the Walecka model and an extended linear sigma model to study the effect of catalysis on the nuclear matter phase transition. In [29], the effects of magnetic field have been studied in the Walecka model by using a weak field approximation of the fermion propagator. The effect of the anomalous magnetic moment of the nucleons are seen to enhance the catalysis effect at zero temperature and zero baryon density [29]. However, at finite temperature, the critical temperature for the vacuum to nuclear matter phase transition for nonzero anomalous magnetic moment of the nucleons, is seen to rise with increasing magnetic field, implying inverse magnetic catalysis [30], whereas for vanishing moments, the behavior is opposite, indicating the magnetic catalysis. Thus, the effect of the anomalous magnetic moments of the nucleons are important to study the contributions from the Dirac sea in presence of finite magnetic field. In the literature there are very few works on the magnetic catalysis effect in the nuclear matter. In our work, we have incorporated this effect within a chiral  $SU(3)$  model, through the magnetized Dirac sea polarizations on the scalar fields.

The open heavy flavor mesons, namely the open charm and the open bottom mesons, have also been studied within the QCD sum rule approach [36–38], the model for composite hadrons [39] and the chiral model, without magnetic field [40, 41], and also with magnetic field [42, 43]. The in-medium masses of the light vector mesons have been studied using the QCD sum rule approach [44], where the medium modifications come through the non-strange and strange light quark condensates and the scalar gluon condensates, calculated within the chiral effective model, in strange asymmetric matter, without the effect of magnetic field [45], and in nuclear medium with the effect of magnetic field [46]. In QCD sum rule approach, the mass modifications of the hidden heavy flavor mesons (charmonium and bottomonium) are found through the medium modifications of the scalar and the twist-2 gluon condensates calculated in a chiral effective model. The open heavy flavor mesons have their mass modifications in terms of both the light quark condensates (because of the light

quark flavor present in their quark structure) as well as gluon condensates simulated within the chiral model. By finding out the mass modifications of the charmonium (bottomonium) and open charm (bottom) mesons within the medium, modifications of their decay widths have also been calculated using a field theoretic model of composite hadrons in presence of magnetic field [32, 47, 48] also using a light quark- anti-quark pair creation model, namely  $^3P_0$  model [49]. These studies have important observable consequences in the relativistic heavy ion collision experiments, with the current focus on the heavy flavor meson in magnetized matter [50–52]. There have also been a numbers of finite temperature studies of heavy quarkonia within the QCD sum rule framework. The properties of strange mesons have been investigated in magnetized matter, within the chiral  $SU(3)$  model [53] and in the field theoretic model [54].

In section II, the chiral  $SU(3)$  model has been described briefly; section III introduces with the Quantum-Chromodynamical (QCD) Sum Rule to find the in-medium masses of the lowest lying quarkonia and the mass shifts of the S-wave states due to the pseudoscalar-vector mesons (PV) mixing in presence of magnetic field; in section IV, the results of the in-medium masses and their shifts at various conditions of nuclear matter are discussed; section V summarizes the findings of this work.

## II. THE CHIRAL $SU(3)_L \times SU(3)_R$ MODEL

In-medium masses of the quarkonium ground states are computed within the QCD sum rule approach, in terms of the gluon condensates. These condensates, in the present study, are calculated in a chiral effective  $SU(3)$  model [55]. The chiral model is based on the non-linear realization of chiral symmetry [56–58], and the scale invariance breaking of QCD [55, 59, 60]. An effective Lagrangian, based on the non-linear realization of chiral symmetry has been employed here, with a logarithmic potential in scalar dilatation field [61],  $\chi$  mimics the scale-invariance breaking of QCD. The chiral  $SU(3)_L \times SU(3)_R$  model Lagrangian density has the following general form [55],

$$\mathcal{L} = \mathcal{L}_{kin} + \mathcal{L}_{BM} + \mathcal{L}_{vec} + \mathcal{L}_0 + \mathcal{L}_{scale-break} + \mathcal{L}_{SB} + \mathcal{L}_{mag} \quad (1)$$

in the above expression,  $\mathcal{L}_{kin}$  is the kinetic energy of the baryons and the mesons;  $\mathcal{L}_{BM}$  represents the baryon-mesons (spin-0 and spin-1) interactions;  $\mathcal{L}_{vec}$ , contains the quartic self-

interactions of the vector mesons and their couplings with the scalar ones;  $\mathcal{L}_0$  incorporates the spontaneous chiral symmetry breaking effects via meson-meson interactions;  $\mathcal{L}_{scale-break}$  is the scale symmetry breaking logarithmic potential; the explicit symmetry breaking term,  $\mathcal{L}_{SB}$ ; finally the magnetic field effects on the charged and neutral baryons in the nuclear medium are given by [19, 20, 42, 43, 62–65],

$$\mathcal{L}_{mag} = -\frac{1}{4}F_{\mu\nu}F^{\mu\nu} - q_i\bar{\psi}_i\gamma_\mu A^\mu\psi_i - \frac{1}{4}\kappa_i\mu_N\bar{\psi}_i\sigma^{\mu\nu}F_{\mu\nu}\psi_i \quad (2)$$

where,  $\psi_i$  is the baryon field operator ( $i = p, n$ ), in the case of nuclear matter, the parameter,  $\kappa_i$  here is related to the anomalous magnetic moment of the  $i$ -th baryon ( $p, n$ ) ([62] - [69]), with  $\kappa_p = 3.5856$  and  $\kappa_n = -3.8263$ , are the gyromagnetic ratio corresponding to the anomalous magnetic moments (AMM) of the proton and the neutron respectively. Thus, in the magnetized nuclear medium, magnetic field has contributed through the Landau energy levels of the charged particles [66], and through the non-zero anomalous magnetic moments of the nucleons [66, 69]. The nucleon self-energy function has modification by the magnetic field dependent Dirac sea contribution and is incorporated within the chiral model through the scalar densities of protons and neutrons in our present work.

In the chiral model, mean-field approximation is adopted, where the meson fields are treated as classical fields. The expectation values of the fields within the system, have non-zero contribution only for the vector (time-component) and scalar meson fields and zero for the other meson (pseudoscalar, axial vector) fields [55].

The scalar dilaton field,  $\chi$  simulates the scalar gluon condensate  $\langle \frac{\alpha_s}{\pi} G_{\mu\nu}^a G^{a\mu\nu} \rangle$ , as well as the twist-2 gluon operator  $\langle \frac{\alpha_s}{\pi} G_{\mu\sigma}^a G_\nu^{a\sigma} \rangle$ , within the model. The energy momentum tensor,  $T_{\mu\nu}$  derived from the  $\chi$ -terms in the chiral model Lagrangian density [13] thus obtained,

$$T_{\mu\nu} = (\partial_\mu\chi) \left( \frac{\partial\mathcal{L}}{\partial(\partial^\nu\chi)} \right) - g_{\mu\nu}\mathcal{L}_\chi \quad (3)$$

The QCD energy momentum tensor, in the limit of current quark masses, contains a symmetric trace-less part and a trace part, as given below [70, 71],

$$T_{\mu\nu} = -ST (G_{\mu\sigma}^a G_\nu^{a\sigma}) + \frac{g_{\mu\nu}}{4} \left( \sum_i m_i \bar{q}_i q_i + \langle \frac{\beta_{QCD}}{2g} G_{\sigma k}^a G_k^{a\sigma} \rangle \right) \quad (4)$$

with the leading order QCD  $\beta$  function [13],  $\beta_{QCD}(g) = -\frac{g^3}{(4\pi)^2}(11 - \frac{2}{3}N_f)$ , by taking the 3 color quantum numbers of QCD, and no. of flavors,  $N_f = 3$ . Here,  $m_i$ 's ( $i = u, d, s$ ) are the

current quark masses.

Writing the medium expectation value of the twist-2 gluon operator as,

$$\left\langle \frac{\alpha_s}{\pi} G_{\mu\sigma}^a G_{\nu}^{a\sigma} \right\rangle = \left( u_\mu u_\nu - \frac{g_{\mu\nu}}{4} \right) G_2 \quad (5)$$

where  $u_\mu$  is the 4-velocity of the nuclear medium, taken to be at rest [13, 14] in the present investigation,  $u_\mu = (1, 0, 0, 0)$ ; the QCD energy momentum tensor then reads

$$T_{\mu\nu} = -\frac{\pi}{\alpha_s} \left( u_\mu u_\nu - \frac{g_{\mu\nu}}{4} \right) G_2 + \frac{g_{\mu\nu}}{4} \left( \sum_i m_i \bar{q}_i q_i + \left\langle \frac{\beta_{QCD}}{2g} G_{\sigma k}^a G_k^{a\sigma} \right\rangle \right) \quad (6)$$

Comparing the expressions of energy momentum tensor in equation(6) and in equation(3), one obtains the expressions for  $G_2$  (the twist-2 component) and the scalar gluon condensate by multiplying both sides with  $(u_\mu u_\nu - \frac{g_{\mu\nu}}{4})$  and  $g^{\mu\nu}$  respectively. These are given by-

$$G_2 = \frac{\alpha_s}{\pi} \left[ - (1 - d + 4k_4)(\chi^4 - \chi_0^4) - \chi^4 \ln \left( \frac{\chi^4}{\chi_0^4} \right) + \frac{4}{3} d \chi^4 \ln \left( \left( \frac{(\sigma^2 - \delta^2)\zeta}{\sigma_0^2 \zeta_0} \right) \left( \frac{\chi}{\chi_0} \right)^3 \right) \right] \quad (7)$$

and,

$$\left\langle \frac{\alpha_s}{\pi} G_{\mu\nu}^a G^{a\mu\nu} \right\rangle = \frac{8}{9} \left[ (1 - d)\chi^4 + \left( \frac{\chi}{\chi_0} \right)^2 \left( m_\pi^2 f_\pi \sigma + \left( \sqrt{2} m_k^2 f_k - \frac{1}{\sqrt{2}} m_\pi^2 f_\pi \right) \zeta \right) \right] \quad (8)$$

Thus, the expectation values of the scalar and the twist-2 gluon condensates depend on the in-medium values of the non-strange scalar field,  $\sigma$ , the strange scalar field,  $\zeta$ , the scalar-isovector field,  $\delta$  [ if the current quark masses are taken to be non-zero ] besides the scalar dilaton field,  $\chi$ , within the chiral  $SU(3)$  model. By deriving the Euler Lagrange's equations of motion from the effective model Lagrangian under mean-field approximation, and taking into account the effect from the magnetized Dirac sea contribution, and the Landau level contribution of the charged Fermi sea of nucleons and the anomalous magnetic moments of the nucleons through the scalar densities of nucleons, the coupled equations of motion of the scalar fields are solved in dense magnetized nuclear matter.

### III. IN-MEDIUM MASSES WITHIN THE QCD SUM RULE APPROACH

In this section, the in-medium masses of the 1S and 1P waves states of heavy-quarkonia [ Charmonium 1S:  $J/\Psi$ ;  $\eta_c$ , 1P:  $\chi_{c0}$  and  $\chi_{c1}$ ; and bottomonium 1S:  $\Upsilon(1S)$ ,  $\eta_b$ ; 1P:  $\chi_{b0}$  and

$\chi_{b1}$  ] are calculated within the QCD Sum Rule approach. In the QCD Sum Rule framework, the masses of these heavy-quarkonia are obtained by using the medium modified scalar and twist-2 gluon condensates. The condensates are then calculated within the chiral SU(3) model in terms of the scalar fields modifications within the magnetized, isospin asymmetric nuclear matter with the additional contribution of the magnetized Dirac sea effects of the nucleons. The in-medium mass squared,  $m_i^{*2}$  for the i-type of quarkonium ( $\bar{q}q$ ;  $q = c, b$ ) ground state [ i= vector, pseudoscalar, scalar, and axial-vector ], in the QCD sum rule can be written as [72],

$$m_i^{*2} \simeq \frac{M_{n-1}^i(\xi)}{M_n^i(\xi)} - 4m_q^2\xi \quad (9)$$

where  $M_n^i$  is the  $n$ -th moment of the i-type meson,  $m_q$  ( $q = c, b$ ) is the running heavy quark mass dependent on the renormalization scale,  $\xi$ . The expressions for the running quark masses are given later. Using the operator product expansion technique [OPE], the moment can be written as [10, 72],

$$M_n^i(\xi) = A_n^i(\xi) [1 + a_n^i(\xi)\alpha_s + b_n^i(\xi)\phi_b + c_n^i(\xi)\phi_c] \quad (10)$$

Here,  $A_n^i, a_n^i, b_n^i$ , and  $c_n^i$  are the Wilson coefficients. The  $A_n^i$  coefficients result from the bare-loop diagram of perturbative QCD,  $a_n^i$  are the contributions from the perturbative radiative corrections, and the coefficients,  $b_n^i$  are related to the scalar gluon condensate through

$$\phi_b = \frac{4\pi^2}{9} \frac{\langle \frac{\alpha_s}{\pi} G_{\mu\nu}^a G^{a\mu\nu} \rangle}{(4m_q^2)^2}. \quad (11)$$

By the replacement of the value of scalar gluon condensate, above equation can be written in terms of the scalar fields as,

$$\phi_b = \frac{32\pi^2}{81(4m_q^2)^2} \left[ (1-d)\chi^4 + \left(\frac{\chi}{\chi_0}\right)^2 \left( m_\pi^2 f_\pi \sigma + \left( \sqrt{2}m_k^2 f_k - \frac{1}{\sqrt{2}}m_\pi^2 f_\pi \right) \zeta \right) \right] \quad (12)$$

Finally, the  $c_n^i$  coefficients are associated with the twist-2 gluon condensates through

$$\phi_c = \frac{4\pi^2}{3(4m_q^2)^2} G_2 \quad (13)$$

In terms of the scalar fields, expression for  $\phi_c$  is,

$$\begin{aligned} \phi_c = & \frac{4\pi\alpha_s}{3(4m_q^2)^2} \left[ - (1-d+4k_4)(\chi^4 - \chi_0^4) - \chi^4 \ln \left( \frac{\chi^4}{\chi_0^4} \right) \right. \\ & \left. + \frac{4}{3} d \chi^4 \ln \left( \left( \frac{(\sigma^2 - \delta^2)\zeta}{\sigma_0^2 \zeta_0} \right) \left( \frac{\chi}{\chi_0} \right)^3 \right) \right] \quad (14) \end{aligned}$$

The  $\xi$ -dependent parameters  $m_q$ , ( $q = c, b$ ) and  $\alpha_s$ , are the running charm and bottom quark masses and the running coupling constant respectively, given below [13, 72],

$$\frac{m_q(\xi)}{m_q} = 1 - \frac{\alpha_s}{\pi} \left[ \frac{2 + \xi}{1 + \xi} \ln(2 + \xi) - 2 \ln 2 \right] \quad (15)$$

with  $m_c(q = c) \equiv m_c(p^2 = -m_c^2) = 1.26$  GeV and  $m_b(q = b) \equiv m_b(p^2 = -m_b^2) = 4.23$  GeV [13, 73], and

$$\alpha_s(Q_0^2 + 4m_q^2) = \alpha_s(4m_q^2) \left/ \left( 1 + \frac{(33 - 2n_f)}{12\pi} \alpha_s(4m_q^2) \ln \frac{Q_0^2 + 4m_q^2}{4m_q^2} \right) \right. \quad (16)$$

where,  $n_f = 4$ ,  $\alpha_s(4m_c^2) \simeq 0.23$  [73] for charm quark sector, and  $n_f = 5$ ,  $\alpha_s(4m_b^2) \simeq 0.15$  [73] in the bottom quark sector;  $Q_0^2 = 4m_q^2\xi$  ( $q = c, b$ ).

The Wilson coefficients  $A_n^i, a_n^i, b_n^i$ , are given in ref.[72] for different quantum numbers,  $J^{PC}$  of particle states, for e.g., the scalar, vector, pseudoscalar, axial-vector channels, etc. The  $c_n^i$ 's are listed for the vector and pseudoscalar channels in [10], in case of S-wave quarkonium ground states, and, for the P-waves (scalar and axial-vector),  $c_n^i$ 's are calculated using a background field technique in Ref. [74].

The mixings of the pseudoscalar ( $P \equiv \eta_c(1S)$ ) and vector ( $V \equiv J/\psi$ ) charmonium states are taken into account through the interaction [32, 34, 38, 39, 54, 75]

$$\mathcal{L}_{PV\gamma} = \frac{g_{PV}}{m_{av}} e \tilde{F}_{\mu\nu} (\partial^\mu P) V^\nu, \quad (17)$$

where  $m_{av} = (m_V + m_P)/2$ ,  $m_P$  and  $m_V$  are the masses for the pseudoscalar and vector charmonium states,  $\tilde{F}_{\mu\nu}$  is the dual electromagnetic field. In the hadronic medium, the charmonium masses are calculated from the medium modification of the dilaton field, using equation (9), within the chiral effective model. In equation (17), the coupling parameter  $g_{PV}$  is fitted from the observed value of the radiative decay width,  $\Gamma(V \rightarrow P + \gamma)$  given as

$$\Gamma(V \rightarrow P\gamma) = \frac{e^2 g_{PV}^2 p_{cm}^3}{12 \pi m_{av}^2}, \quad (18)$$

where,  $p_{cm} = (m_V^2 - m_P^2)/(2m_V)$  is the magnitude of the center of mass momentum in the final state. The masses of the pseudoscalar and the longitudinal component of the vector mesons including the mixing effects are given by

$$m_{P,V||}^2 = \frac{1}{2} \left( M_+^2 + \frac{c_{PV}^2}{m_{av}^2} \mp \sqrt{M_-^4 + \frac{2c_{PV}^2 M_+^2}{m_{av}^2} + \frac{c_{PV}^4}{m_{av}^4}} \right), \quad (19)$$



where  $M_+^2 = m_P^2 + m_V^2$ ,  $M_-^2 = m_V^2 - m_P^2$  and  $c_{PV} = g_{PV}eB$ . By considering the terms in equation (19) up to the second order in  $c_{PV}$  and leading order in  $(m_V - m_P)/2m_{av}$ , we obtain

$$m_{P,V||}^2 (PV) = m_{P/V}^2 \mp \frac{c_{PV}^2}{M_-^2} \quad (20)$$

The effective Lagrangian term given by equation (17) has been observed to lead to the mass modifications of the longitudinal  $J/\psi$  and  $\eta_c$  due to the presence of the magnetic field, which agree extremely well with a study of these charmonium states using a QCD sum rule approach incorporating the mixing effects [34, 75]. In the present study, we have incorporated the effects from the magnetic field modified Dirac sea polarizations apart from the Landau level contributions of the Fermi sea of protons in the nuclear matter, on the mixing effects between the longitudinal component of vector charmonium,  $(J/\Psi^{\parallel})$  and pseudoscalar charmonium ( $\eta_c$ ) with their masses,  $m_V$  and  $m_P$  calculated from the QCD sum rule approach. The effects of spin-magnetic field interaction have been studied for the 1S charmonium states, vector  $J/\Psi$  and pseudoscalar  $\eta_c$  at finite magnetic fields [14, 34, 75–77]. This leads to a mixing between  $J/\Psi^{\parallel}$  (1S) and  $\eta_c$  states.

In the presence of an external magnetic field, we have considered the effects of spin-magnetic field interaction on the bottomonium 1S triplet and singlet states. At non-zero magnetic fields, the spin-magnetic field coupling leads to a mixing between the longitudinal component of the spin one ( $\Upsilon^{\parallel}(1S)$ ) state and the spin zero ( $\eta_b$ ) state. The masses of the longitudinal vector,  $\Upsilon^{\parallel}(1S)$  (pseudoscalar,  $\eta_b$ ) bottomonium states, are seen to have a rise (drop) with increasing magnetic fields, when the spin-mixing effects are incorporated at finite magnetic fields both including the magnetized Dirac sea polarizations and without including this effect in the nuclear matter. The effective masses of the  $\Upsilon^{\parallel}(1S)$  and  $\eta_b$ , by considering the shifts due to spin-magnetic field interaction,  $-\mu \cdot B$  [76] (due to the lack of experimental data on the bottomonium radiative decay width,  $\Upsilon(1S) \rightarrow \eta_b \gamma$ ), are given by

$$m_{\Upsilon(1S)}^{eff} = m_{\Upsilon(1S)}^* + \Delta m_{sB}, \quad m_{\eta_b}^{eff} = m_{\eta_b}^* - \Delta m_{sB} \quad (21)$$

In the above equation,  $m_{\Upsilon(1S)/\eta_b}^*$  denotes the in-medium masses of the S-waves bottomonium ground states calculated within QCD sum rule framework [equation. (9)], and  $\Delta m_{sB}$  is the shift due to the spin-magnetic field interaction. Expression for the latter is given as below,

$$\Delta m_{sB} = \frac{\Delta M}{2} \left( (1 + \chi_{sB}^2)^{1/2} - 1 \right), \quad \chi_{sB} = \frac{2g\mu_b B}{\Delta M} \quad (22)$$

where,  $\mu_b = (\frac{1}{3}e)/(2m_b)$  is the bottom quark Bohr magneton with the constituent bottom quark mass,  $m_b = 4.7$  GeV [76],  $\Delta M = m_{\Upsilon}^* - m_{\eta_b}^*$ , and  $g$  is chosen to be 2 (ignoring the effects of the anomalous magnetic moments of the bottom quark (anti-quark)).

## IV. RESULTS AND DISCUSSIONS

### A. Charmonium states

In this subsection, the results on the in-medium masses of the lowest S-wave:  $J/\psi$  ( $^3S_1$ ) and  $\eta_c$  ( $^1S_0$ ) and P-wave:  $\chi_{c0}$  ( $^3P_0$ ) and  $\chi_{c1}$  ( $^3P_1$ ), charmonium states are discussed in the presence of magnetized, isospin asymmetric, nuclear matter with the additional contribution of the magnetized Dirac sea effects of nucleons. The masses are found in the QCD sum rule framework by calculating the moments ( $M_n^i$ ) for all the four channels of vector ( $^3S_1$ ), pseudoscalar ( $^1S_0$ ), scalar ( $^3P_0$ ) and axial-vector ( $^3P_1$ ) currents. The moments are given in terms of the perturbative Wilson coefficients and the non-perturbative gluon condensates terms. These coefficients are different for the different quantum numbers of current channels and are independent of any medium effects. The masses are also dependent on the running charm quark mass ( $m_c(\xi)$ ) and the running coupling constant ( $\alpha_s(\xi)$ ), which are dependent on the renormalization scale  $\xi$ . The scalar gluon condensate,  $\langle \frac{\alpha_s}{\pi} G_{\mu\nu}^a G^{a\mu\nu} \rangle$  through the  $\phi_b$  term and the twist-2 gluon condensate,  $G_2$  in  $\phi_c$  term incorporate the effects of density, magnetic fields and isospin asymmetry of the nuclear medium on the charmonium masses. The gluon condensates are determined in the chiral effective model using the mean field approximation, in which the meson fields are treated as classical fields. In the presence of an external strong magnetic field, the proton has contributions from the Landau energy levels. The nucleons also can have contributions through their anomalous magnetic moments on the meson masses at finite magnetic fields. In the present investigation, we have studied the magnetized Dirac sea contributions leading to the magnetic catalysis effects, on the charmonium masses. The nucleon self-energy function is found from the interaction Lagrangian of the scalar fields and nucleon within the chiral  $SU(3)$  model. The self-energy of the nucleon can be evaluated using the Feynman tadpole diagrams for nucleons. The nucleon propagators get modified in presence of a finite magnetic field and additional effects can be obtained due to the anomalous magnetic moments of the nucleons. The scalar densities of the protons

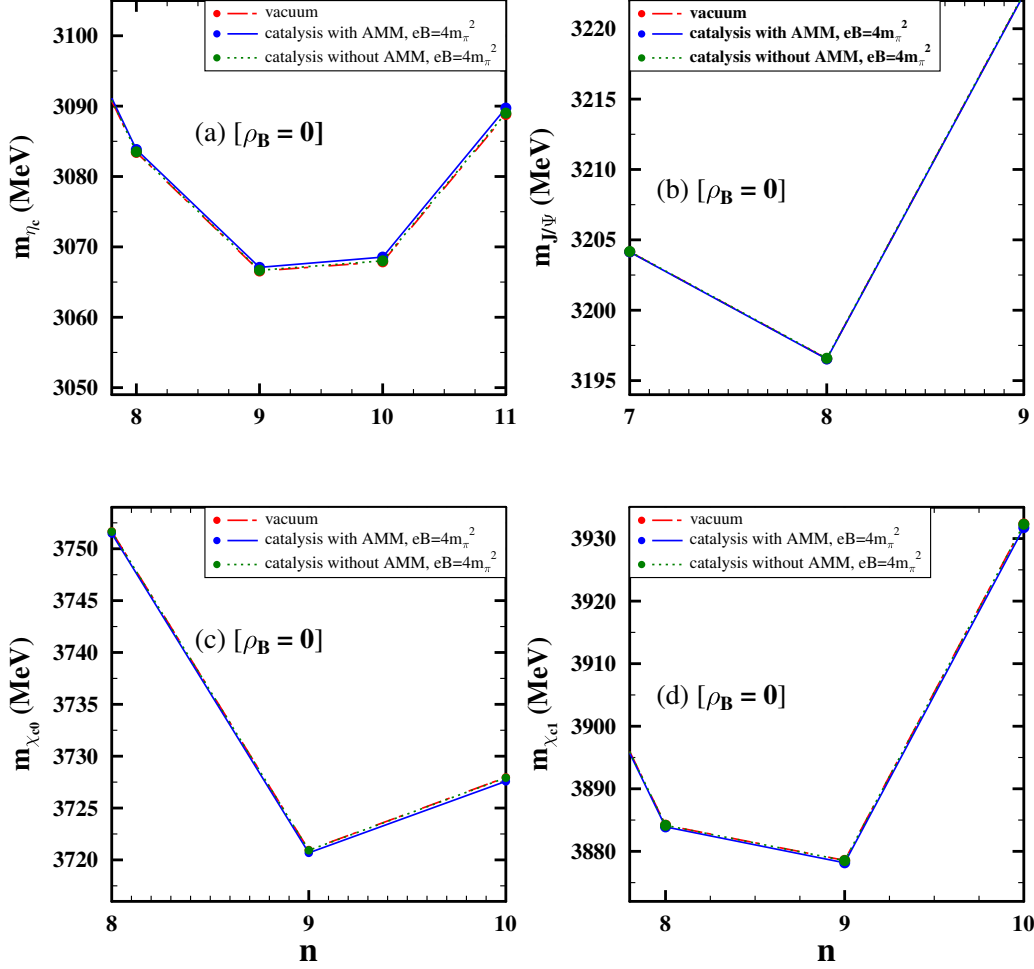


FIG. 1: Masses (MeV) are plotted as a function of  $n$ , for 1S ( $J/\psi$ ,  $\eta_c$ ) and 1P ( $\chi_{c0}$  and  $\chi_{c1}$ ) states, at  $\rho_B = 0$ . The magnetized Dirac sea effects have contributions at zero density and are shown for  $eB = 4m_\pi^2$ , with and without nucleon AMM effects (Vacuum masses correspond to the minimum point of the dot-dashed line).

( $\rho_p^s$ ) and neutrons ( $\rho_n^s$ ) have contributions from this magnetized Dirac sea effects in addition to the mean-field contributions of the Fermi sea of nucleons. For the given values of baryon density,  $\rho_B$ , isospin asymmetry,  $\eta = (\rho_n - \rho_p)/(2\rho_B)$  ( $\rho_p$  and  $\rho_n$  are the number densities of proton and neutron, respectively), and magnetic field, the scalar fields are solved from their coupled equations of motion considering the effects of magnetized Fermi and Dirac sea of nucleons. The twist-2 and the scalar gluon condensates, are calculated from equations (7)

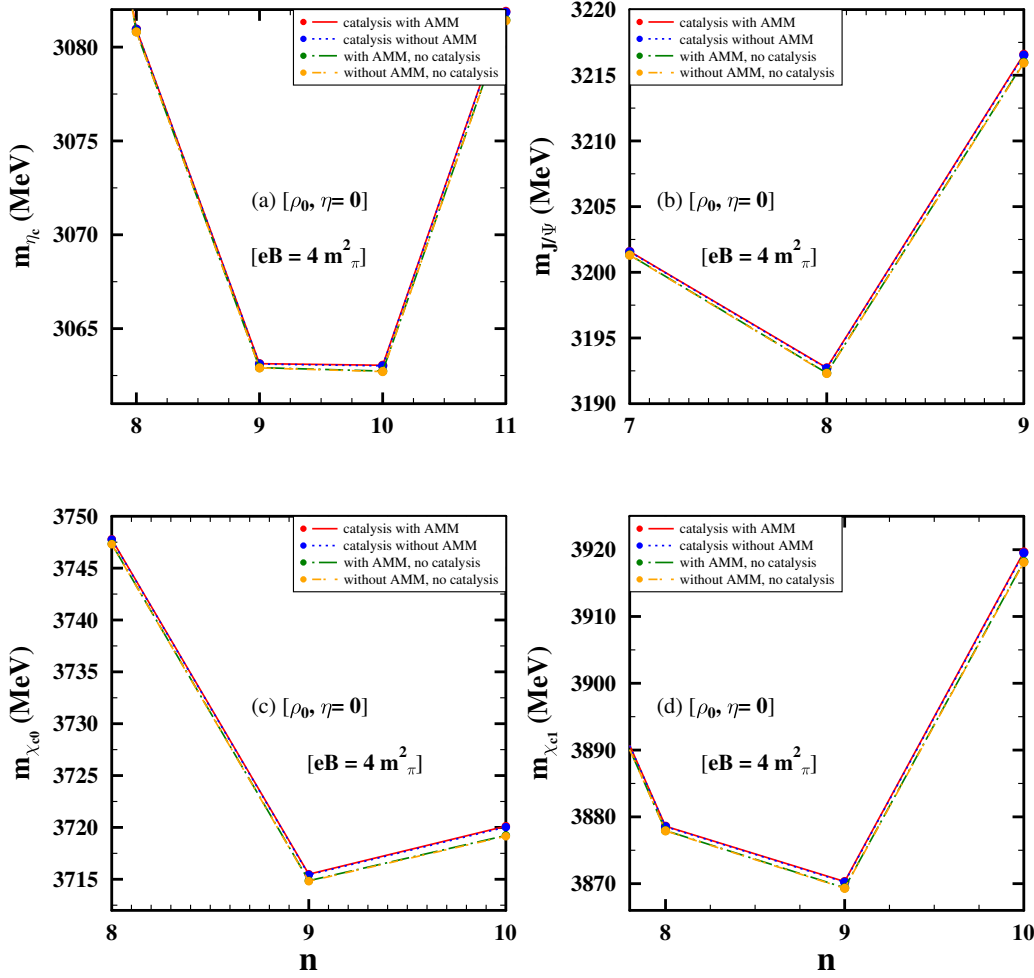


FIG. 2: Masses (MeV) are plotted as a function of  $n$ , for 1S ( $J/\psi$  and  $\eta_c$ ) and 1P states ( $\chi_{c0}$  and  $\chi_{c1}$ ) at  $\rho_B = \rho_0$  and  $\eta = 0$ . The effects of magnetized Dirac sea at  $eB = 4m_\pi^2$  are shown along with the case when only Landau level contributions of protons are taken into account. Plots are made with and without AMM effects of nucleons.

and (8), which are then used to calculate the values of  $\phi_b$  and  $\phi_c$  (given by Eqs. (12) and (14) respectively). Using the values of  $\phi_b$  and  $\phi_c$ , the in-medium charmonium masses are calculated using equation (9). For the S-wave charmonium states, in presence of an external magnetic field, the mixing between the vector and pseudoscalar mesons are also considered in a phenomenological Lagrangian approach to calculate the effective masses for  $J/\psi^{\parallel}$  and  $\eta_c$ , using equation (20).

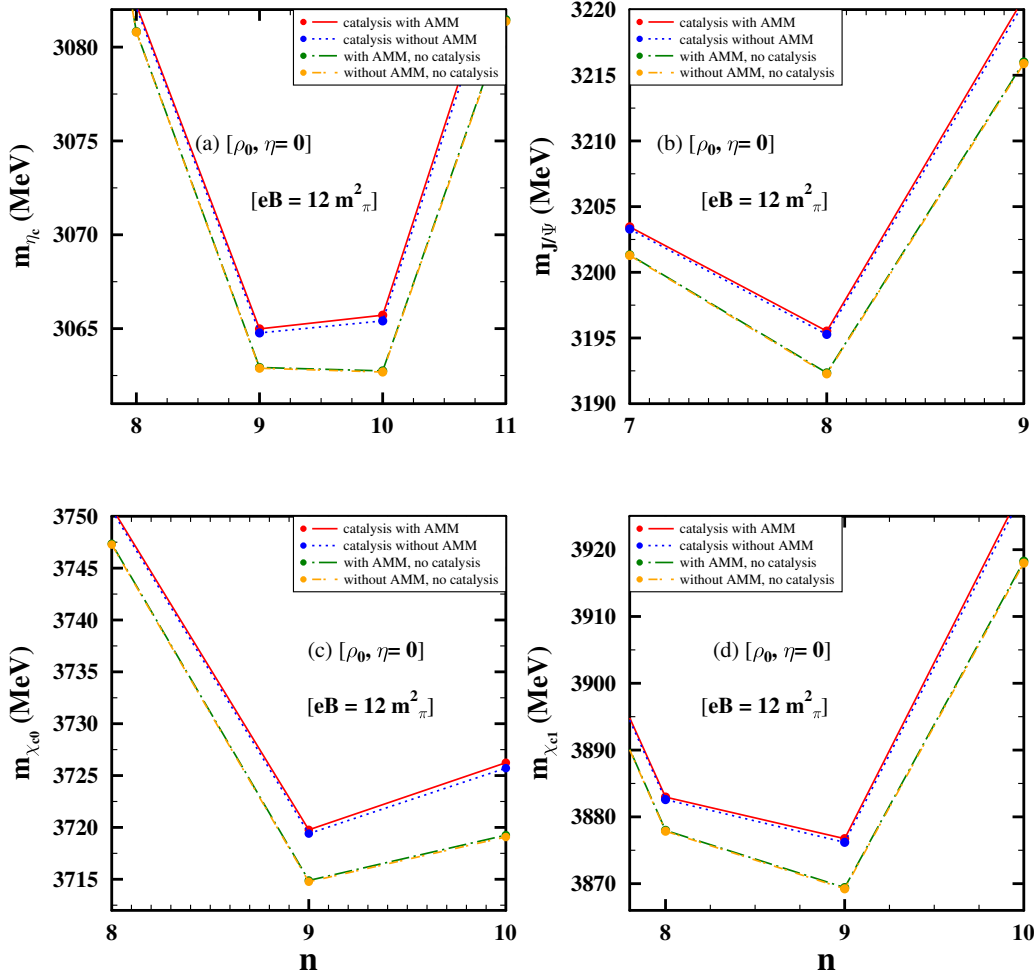


FIG. 3: Masses (MeV) are plotted as a function of  $n$ , for 1S ( $J/\psi$  and  $\eta_c$ ) and 1P states ( $\chi_{c0}$  and  $\chi_{c1}$ ) at  $\rho_B = \rho_0$  and  $\eta = 0$ . The effects of magnetized Dirac sea at  $eB = 12m_\pi^2$  are shown by comparing with the masses when this effect is not considered over the Landau level contributions of protons. Plots are made with and without AMM effects of nucleons.

The nuclear matter saturation density,  $\rho_0$  is taken to be  $0.15 \text{ fm}^{-3}$  in our present investigation. The value of the renormalization scale,  $\xi = 1$  is chosen for the S-wave charmonium states and  $\xi = 2.5$  is taken for the P-wave charmonium states to study their respective in-medium masses. These choices lead to the  $\xi$  dependent coupling constant and charm quark mass,  $\alpha_s = 0.21$  and  $m_c = 1.24 \text{ GeV}$  for the S-wave mass calculations and  $\alpha_s = 0.1948$  and  $m_c = 1.22 \text{ GeV}$  for the P-wave mass calculations, respectively. With these parameters and

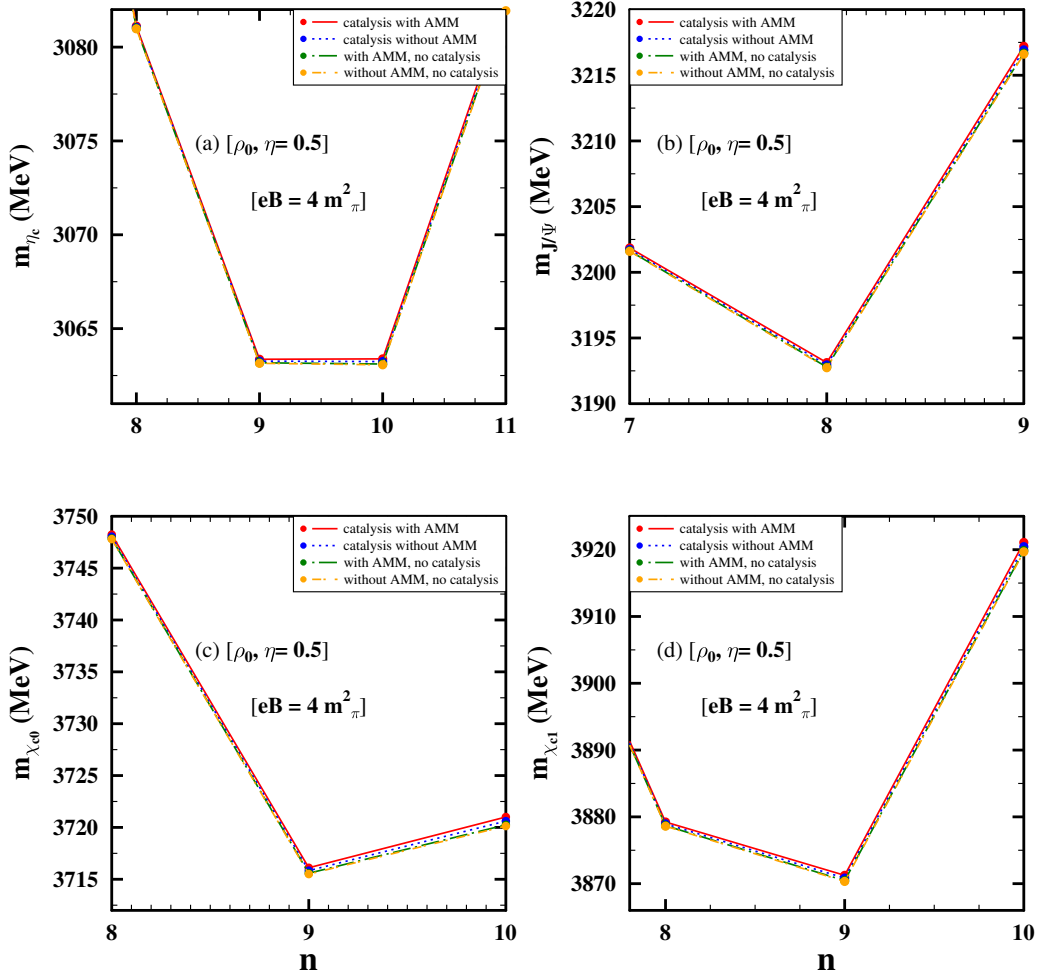


FIG. 4: Masses (MeV) are plotted as a function of  $n$ , for 1S ( $J/\psi$  and  $\eta_c$ ) and 1P states ( $\chi_{c0}$  and  $\chi_{c1}$ ) at  $\rho_B = \rho_0$  and  $\eta = 0.5$ . The effects of magnetized Dirac sea at  $eB = 4m_\pi^2$  are shown along with the case when only Landau level contributions of protons are taken into account. Plots are made with and without AMM effects of nucleons.

with  $\phi_b$  calculated within the chiral effective model, the vacuum masses (in MeV) of  $J/\psi$  and  $\eta_c$  are obtained to be 3196.56 and 3066.57 respectively. The vacuum masses (in MeV) of  $\chi_{c0}$  and  $\chi_{c1}$  are obtained as 3720.95 and 3878.55 respectively. The scalar fields are solved with and without the magnetized Dirac sea contributions at finite magnetic field along with the Landau level contribution of protons and the non zero anomalous magnetic moments (AMM) of the nucleons at finite density. However, at zero density and finite magnetic field,

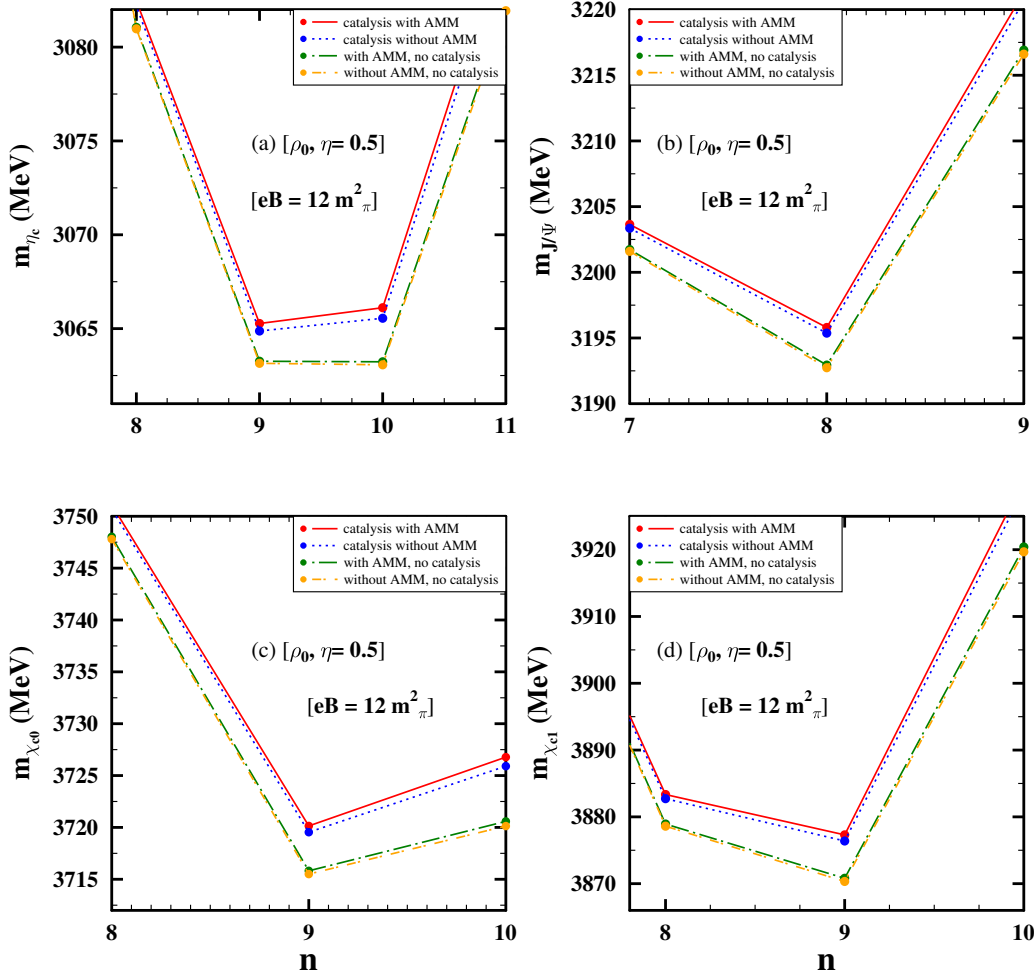


FIG. 5: Masses (MeV) are plotted as a function of  $n$ , for 1S ( $J/\psi$  and  $\eta_c$ ) and 1P states ( $\chi_{c0}$  and  $\chi_{c1}$ ) at  $\rho_B = \rho_0$  and  $\eta = 0.5$ . The effects of magnetized Dirac sea on the masses, at  $eB = 12m_\pi^2$  are shown by comparing with the case when this effect is not considered over the Landau level contributions of protons. Plots are made with and without AMM effects of nucleons.

there will be no contribution from the matter part through Landau quantization, but the vacuum polarizations of the nucleons give rise to some non trivial effects on the scalar fields. The coupled equations of motion for the scalar fields are solved at zero density,  $\rho_B = 0$ , taking into account the magnetized vacuum polarizations of nucleons both for the zero and non-zero anomalous magnetic moments of the protons and neutrons. The values of the scalar fields associated to the QCD vacuum condensates, tend to rise with magnetic field, give rise

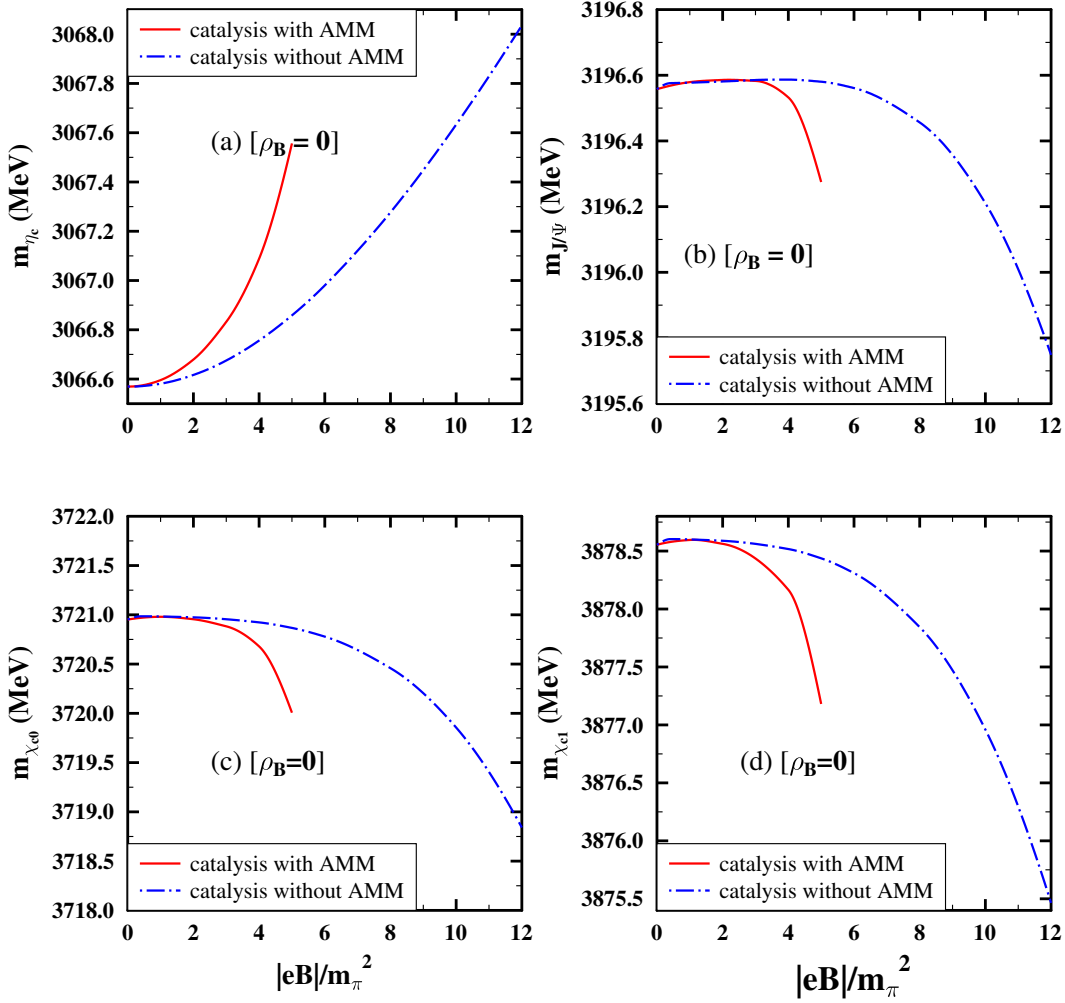


FIG. 6: Masses (MeV) are plotted as a function of  $|eB|$  (in units of  $m_\pi^2$ ) for 1S- ( $J/\psi$  and  $\eta_c$ ) and 1P- ( $\chi_{c0}$  and  $\chi_{c1}$ ) wave states of charmonia, at  $\rho_B = 0$ . At zero density, the variation in masses with magnetic field are only coming from the magnetized Dirac sea polarizations. There is no effect from Landau level quantization of protons or AMM effects of nucleons of the matter part at  $\rho_B = 0$ .

to the effect called magnetic catalysis. The solutions for the scalar fields are given up to  $eB = 5.5 m_\pi^2$  at zero density and when the anomalous magnetic moments of the nucleons are taken into account.

In-medium masses of the 1S and 1P charmonia are thus computed within the sum rule approach by using the scalar and twist-2 gluon condensates in terms of the scalar fields



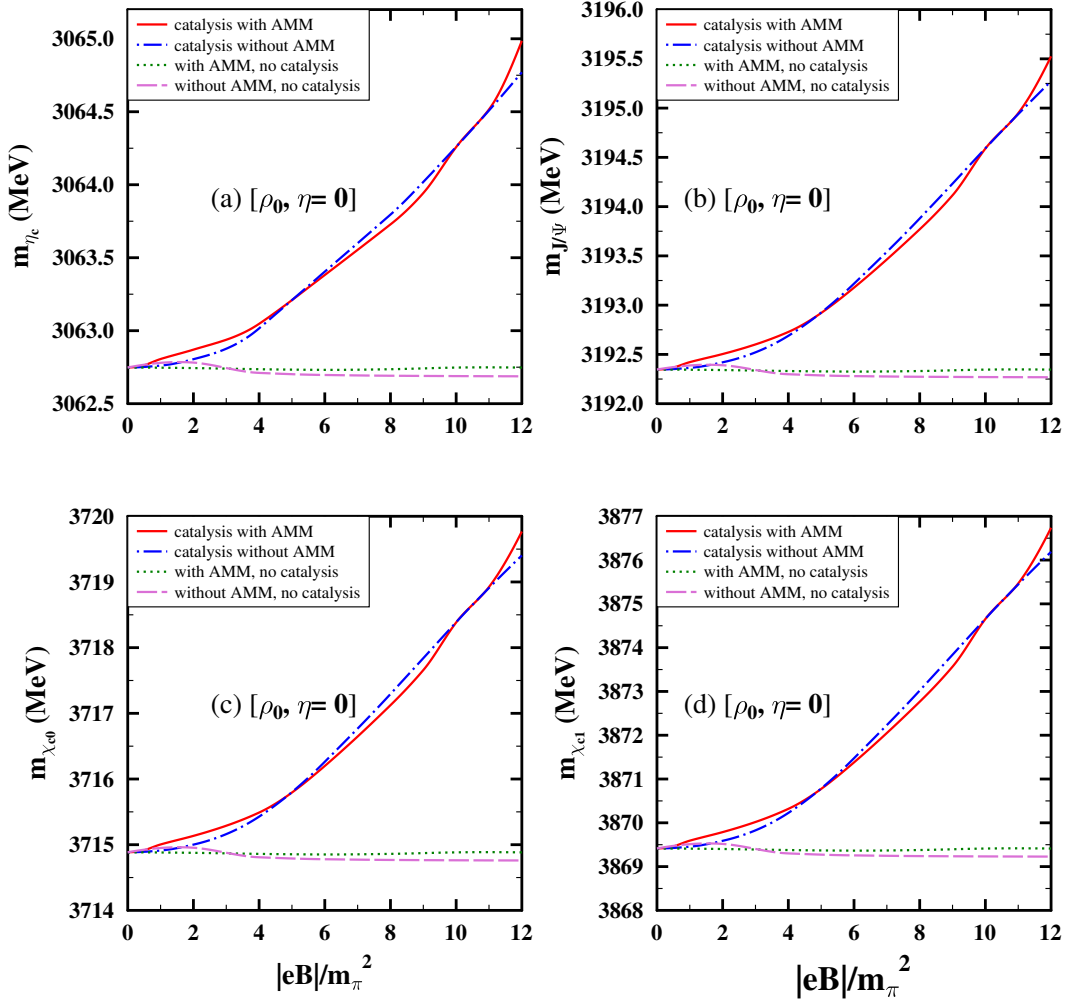


FIG. 7: Masses (MeV) are plotted as a function of  $|eB|$  (in units of  $m_\pi^2$ ) for 1S ( $J/\psi$  and  $\eta_c$ ) and 1P ( $\chi_{c0}$  and  $\chi_{c1}$ ) charmonium states at  $\rho_B = \rho_0$  and  $\eta = 0$ . The masses are computed incorporating the magnetized Dirac sea contribution, show the magnetic catalysis effect (solid line with AMM and dot-dashed line without AMM). Masses are compared to the case when only Landau level contributions of Fermi sea are considered (dotted line with AMM and long-dashed line for without AMM).

calculated in the chiral  $SU(3)$  model. In Fig.1, masses of all the four states are plotted as a function of the order of the moment,  $n$ . The value of  $n$  correspond to the minimum point gives the physical mass of the associated state. In this work, the masses plotted incorporating the effects of magnetized Dirac sea, are denoted as "catalysis with AMM" when the

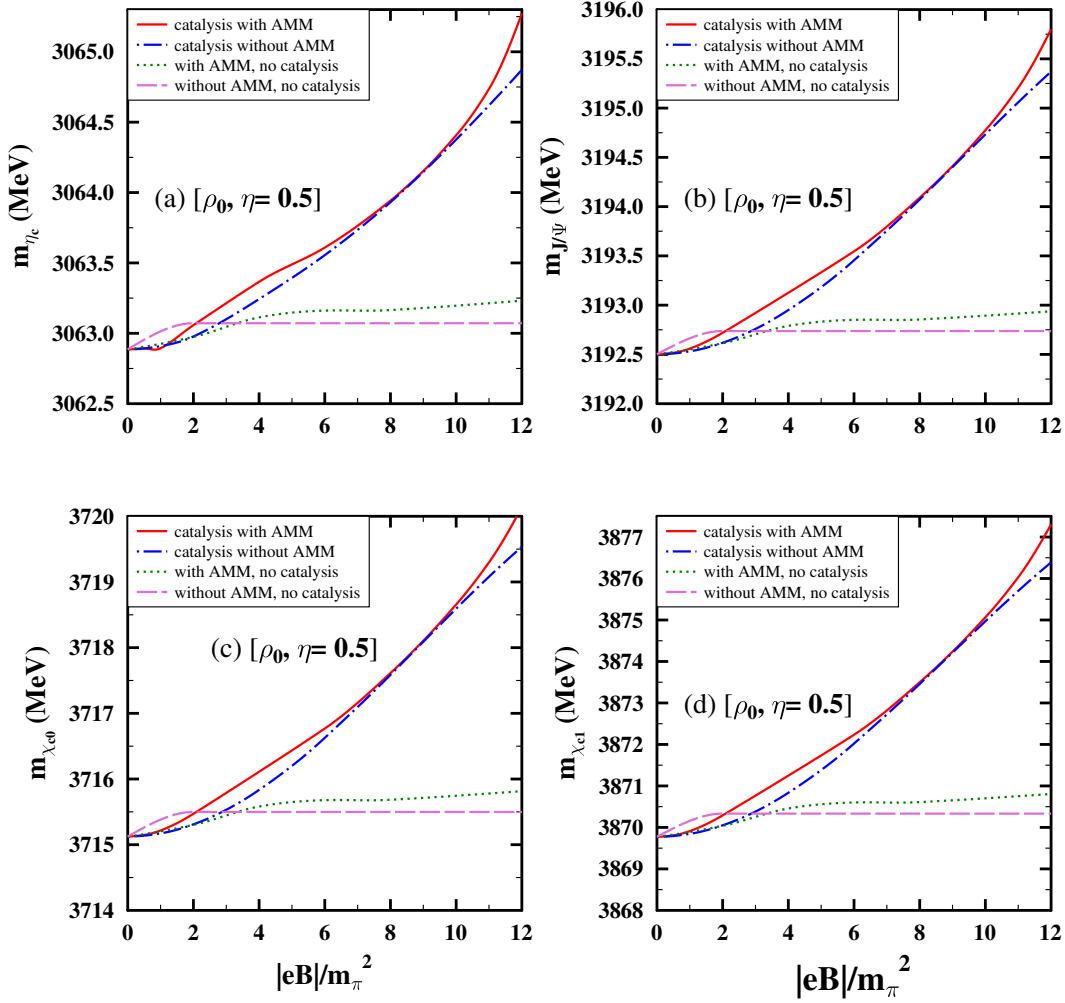


FIG. 8: Masses (MeV) are plotted as a function of  $|eB|$  (in units of  $m_\pi^2$ ) for 1S ( $J/\psi$  and  $\eta_c$ ) and 1P ( $\chi_{c0}$  and  $\chi_{c1}$ ) charmonium states at  $\rho_B = \rho_0$  and  $\eta = 0.5$ . The masses are computed incorporating the magnetized Dirac sea contribution, show the magnetic catalysis effect (solid line with AMM and dot-dashed line without AMM). Masses are compared to the case when only Landau level contributions of Fermi sea are considered (dotted line with AMM and long-dashed line for without AMM).

anomalous magnetic moments of the nucleons are considered and "catalysis without AMM" when not considered. In Figs.[2-5], the in-medium masses of the 1S-wave and 1P-wave states are plotted as a function of  $n$ , at nuclear matter saturation density,  $\rho_B = \rho_0$  for symmetric ( $\eta = 0$ ) as well as asymmetric ( $\eta = 0.5$ ) nuclear matter and at magnetic field values of

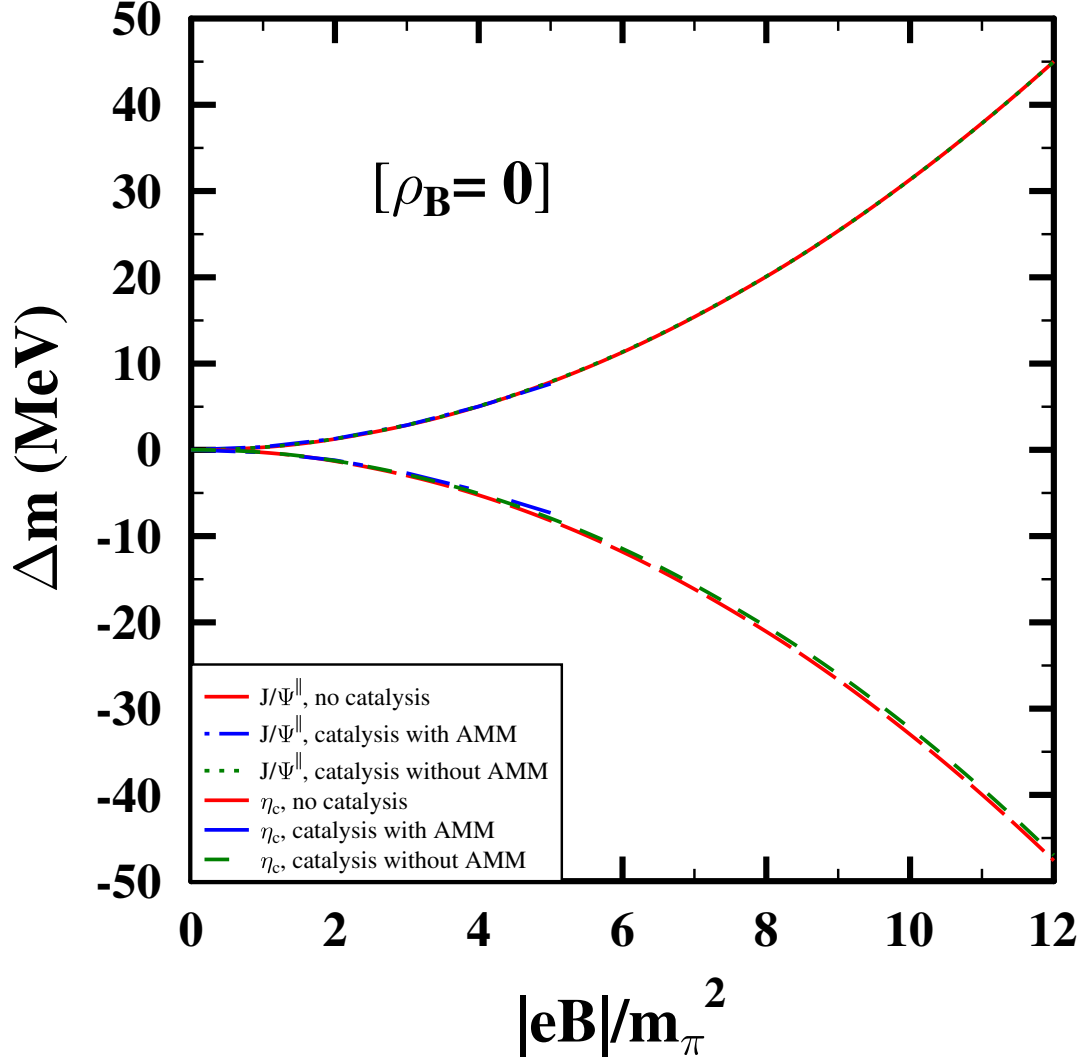


FIG. 9: Mass shifts (in MeV) are plotted as a function of  $|eB|$  (in units of  $m_\pi^2$ ) by considering the mixing between the longitudinal component of  $J/\psi$  and  $\eta_c$ . Mixing effects are calculated with and without magnetized Dirac sea polarizations at  $\rho_B = 0$ .

$eB = 4, 12m_\pi^2$ . As can be seen from Fig.3 and Fig.5, the anomalous magnetic moments of the nucleons have distinguishable contribution on the masses in the case of catalysis effect as compared to the no catalysis case (when there is no Dirac sea contribution). In order to see the importance of the magnetic catalysis on the charmonium masses, Figs.[7-8] illustrate the variation of mass with magnetic field and compare the two situations, when the magnetic

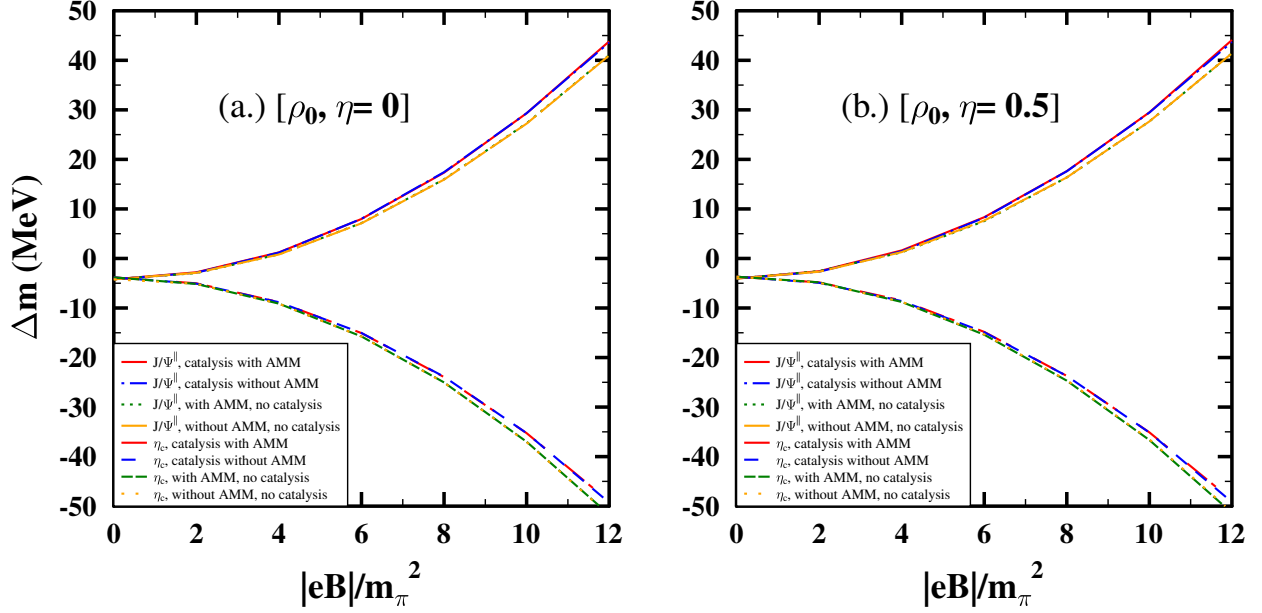


FIG. 10: Mass shifts (in MeV) are plotted as a function of  $|eB|$  (in units of  $m_\pi^2$ ) by considering the mixing between the longitudinal component of  $J/\psi$  and  $\eta_c$ . Mixing effects are calculated with and without magnetized Dirac sea polarizations at  $\rho_B = \rho_0$ , in plot (a.) for symmetric nuclear matter ( $\eta = 0$ ) and plot (b.) for asymmetric matter ( $\eta = 0.5$ ).

field modified Dirac sea polarizations are taken into account along with the Fermi sea effects and when magnetic field contributions are only on the nucleon Fermi sea through protons Landau levels and non-zero AMMs of the nucleons. The masses of the four lowest states of charmonia increase with magnetic field at  $\rho_B = \rho_0$  and  $\eta = 0, 0.5$  for the case of magnetic catalysis. But there is no significant variation in the masses without catalysis effect. In Fig.6, the mass variation with magnetic field are shown for zero density,  $\rho_B = 0$ . The effects of anomalous magnetic moments is observed to be important on the charmonium masses at zero density. The different behavior of the pseudoscalar meson mass with magnetic field in the absence of nuclear matter, can be attributed to the variation in the Wilson coefficients for different channels.

The mixing between the longitudinal component of the vector meson,  $J/\Psi^{\parallel}$  and the pseudoscalar meson,  $\eta_c$  is also studied in the present work using a phenomenological Lagrangian approach. The parameter  $g_{PV} \equiv g_{\eta_c J/\psi}$  is evaluated to be 2.094 from the observed radiative decay width  $\Gamma(J/\psi \rightarrow \eta_c \gamma)$  in vacuum of 92.9 keV [78], using equation (18). This effect gives rise to increasing (decreasing) mass of the  $J/\Psi^{\parallel}$  ( $\eta_c$ ) with magnetic field. In Figs.[9-10] mass shifts of the  $J/\Psi^{\parallel}$  and  $\eta_c$  are plotted as a function of eB at  $\rho_B = 0$  and  $\rho_B = \rho_0$  for  $\eta = 0, 0.5$  incorporating the  $PV$  mixing effect in presence of magnetic field both taking into account the catalysis effect and without this effect.

## B. Bottomonium states

In this section, the results on the in-medium masses of the lowest S-wave:  $\Upsilon(1S)$  ( $^3S_1$ ) and  $\eta_b$  ( $^1S_0$ ) and P-wave:  $\chi_{b0}$  ( $^3P_0$ ) and  $\chi_{b1}$  ( $^3P_1$ ), bottomonium states are discussed in the presence of magnetized, isospin asymmetric, nuclear matter with the additional contribution of the magnetized Dirac sea effects of nucleons. The masses are found in the QCD sum rule framework by calculating the moments ( $M_n^i$ ) for all the four channels of vector ( $^3S_1$ ), pseudoscalar ( $^1S_0$ ), scalar ( $^3P_0$ ) and axial-vector ( $^3P_1$ ) currents. The moments are given in terms of the perturbative Wilson coefficients and the non-perturbative gluon condensates terms. These coefficients are different for the different quantum numbers of current channels and are independent of any medium effects. The masses are also dependent on the running bottom quark mass ( $m_b(\xi)$ ) and the running coupling constant ( $\alpha_s(\xi)$ ), which are dependent on the renormalization scale  $\xi$ . The scalar gluon condensate,  $\langle \frac{\alpha_s}{\pi} G_{\mu\nu}^a G^{a\mu\nu} \rangle$  through the  $\phi_b$  term and the twist-2 gluon condensate,  $G_2$  in  $\phi_c$  term incorporate the effects of density, magnetic fields and isospin asymmetry of the nuclear medium on the bottomonium masses. The gluon condensates are determined in the chiral effective model using the mean field approximation, in which the meson fields are treated as classical fields. In the presence of an external strong magnetic field, the proton has contributions from the Landau energy levels. The nucleons also can have contributions through their anomalous magnetic moments on the meson masses at finite magnetic fields. In the present investigation, we have studied the magnetized Dirac sea contributions leading to the magnetic catalysis effects, on the bottomonium masses. The nucleon self-energy function is found from the interaction Lagrangian of the scalar fields and nucleon within the chiral  $SU(3)$  model. The self-energy of the nucleon can

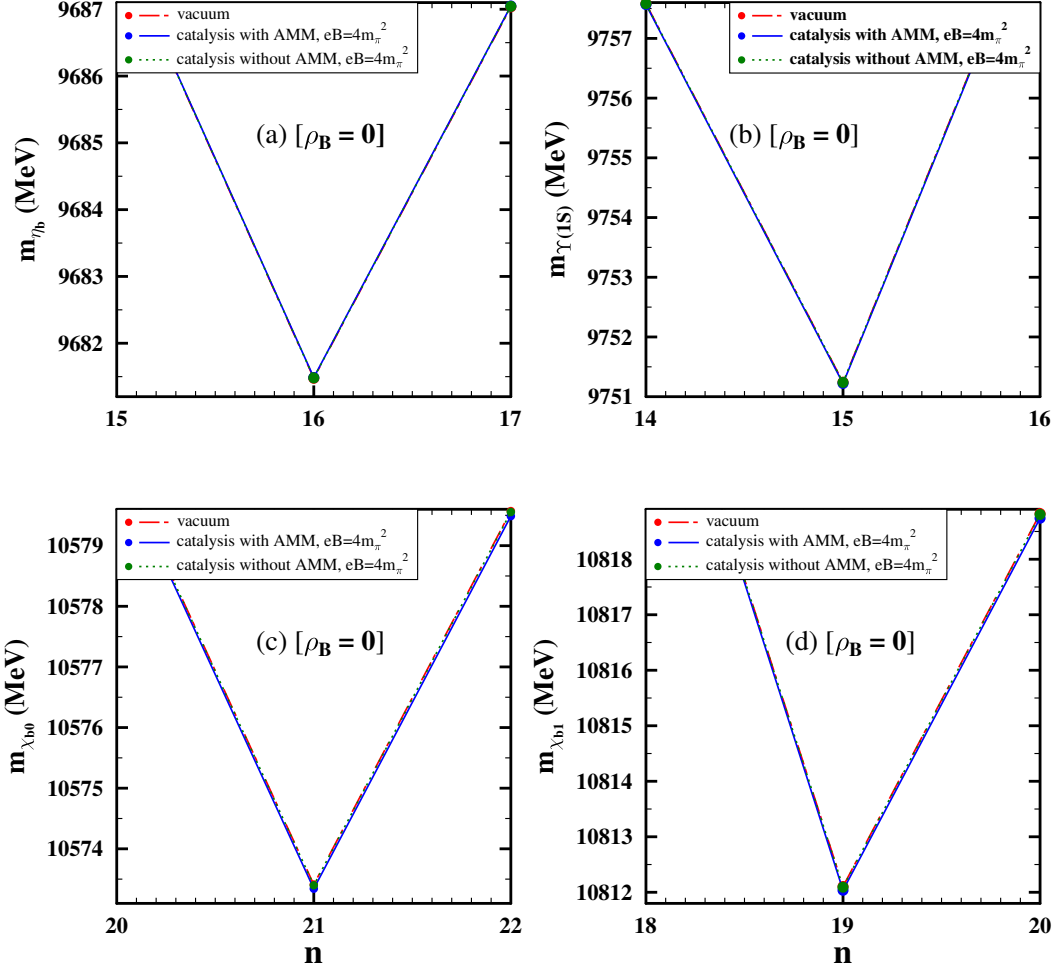


FIG. 11: Masses (MeV) are plotted as a function of  $n$ , for 1S ( $\Upsilon(1S)$  and  $\eta_b$ ) and 1P ( $\chi_{b0}$  and  $\chi_{b1}$ ) bottomonium states, at  $\rho_B = 0$ . The magnetized Dirac sea effects have contributions at zero density and are shown for  $eB = 4m_\pi^2$ , with and without nucleon AMM effects (Vacuum masses correspond to the minimum point of the dot-dashed line).

be evaluated using the Feynman tadpole diagrams for nucleons. The nucleon propagators get modified in presence of a finite magnetic field and additional effects can be obtained due to the anomalous magnetic moments of the nucleons. The scalar densities of the protons ( $\rho_p^s$ ) and neutrons ( $\rho_n^s$ ) have contributions from this magnetized Dirac sea effects in addition to the mean-field contributions of the Fermi sea of nucleons. For the given values of baryon density,  $\rho_B$ , isospin asymmetry,  $\eta = (\rho_n - \rho_p)/(2\rho_B)$  ( $\rho_p$  and  $\rho_n$  are the number densities

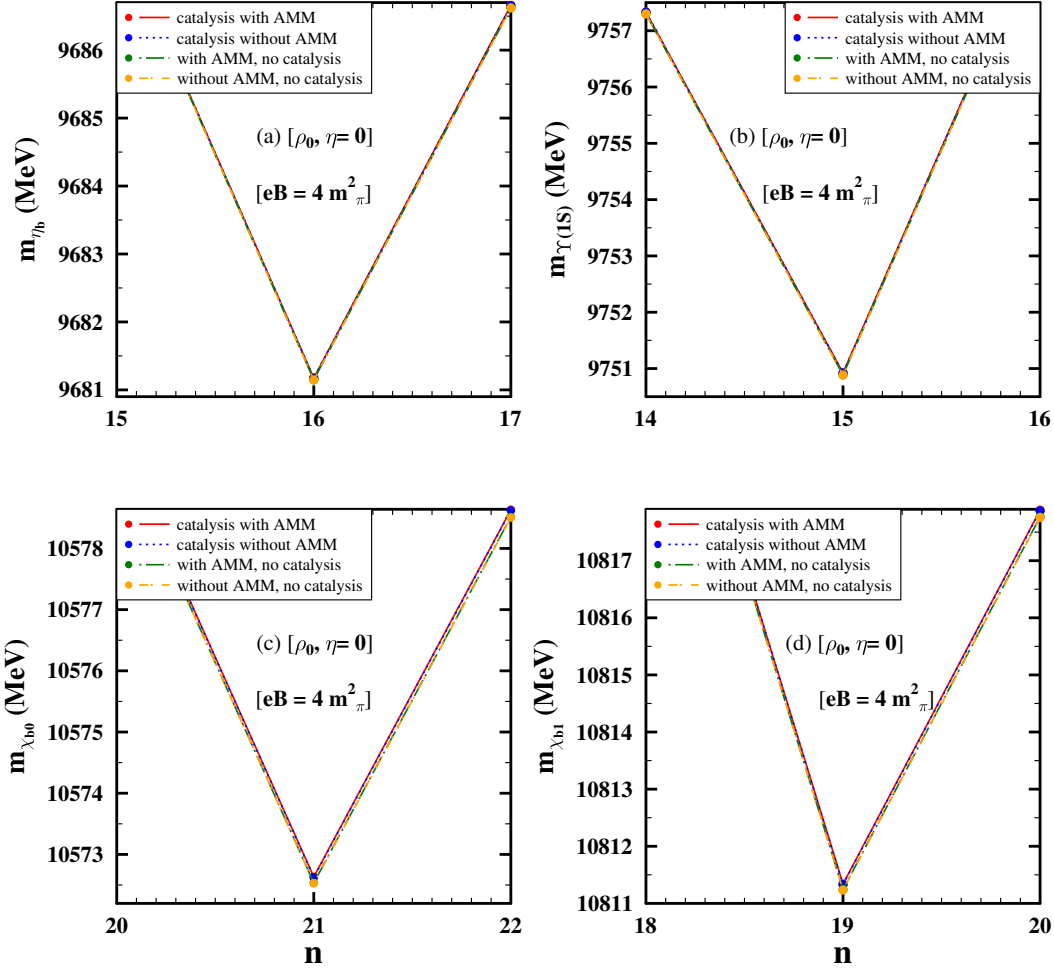


FIG. 12: Masses (MeV) are plotted as a function of  $n$ , for 1S ( $\Upsilon(1S)$  and  $\eta_b$ ) and 1P ( $\chi_{b0}$  and  $\chi_{b1}$ ) bottomonium at  $\rho_B = \rho_0$  and  $\eta = 0$ . The effects of magnetized Dirac sea at  $eB = 4m_\pi^2$  are shown along with the case when only Landau level contributions of protons are taken into account. Plots are made with and without AMM effects of nucleons.

of proton and neutron, respectively), and magnetic field, the scalar fields are solved from their coupled equations of motion considering the effects of magnetized Fermi and Dirac sea of nucleons. The twist-2 and the scalar gluon condensates, are calculated from equations (7) and (8), which are then used to calculate the values of  $\phi_b$  and  $\phi_c$  (given by equations (12) and (14) respectively). Using the values of  $\phi_b$  and  $\phi_c$ , the in-medium masses of the bottomonium are calculated using Eq. (9). For the S-wave bottomonium states, the effects

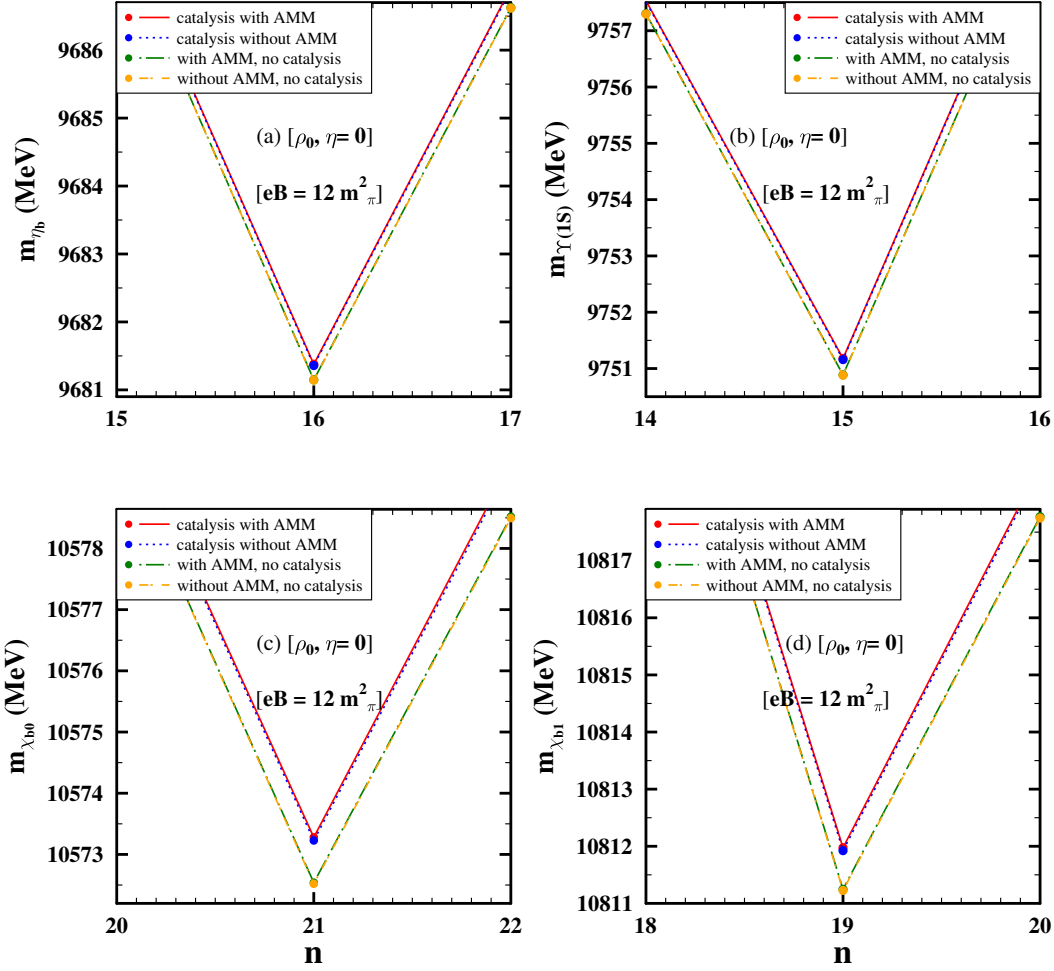


FIG. 13: Masses (MeV) are plotted as a function of  $n$ , for 1S ( $\Upsilon(1S)$  and  $\eta_b$ ) and 1P ( $\chi_{b0}$  and  $\chi_{b1}$ ) bottomonium states at  $\rho_B = \rho_0$  and  $\eta = 0$ . The effects of magnetized Dirac sea at  $eB = 12m_\pi^2$  are shown by comparing with the masses when this effect is not considered over the Landau level contributions of protons. Plots are made with and without AMM effects of nucleons.

of the spin-magnetic field interaction are also considered using a Hamiltonian approach to calculate the effective masses for  $\Upsilon(1S)$  and  $\eta_b$ , using Eq. (21).

Similar to the charmonium sector, the value of the renormalization scale,  $\xi = 1$  is chosen for the S-wave states and  $\xi = 2.5$  is taken for the P-wave states to study their respective in-medium masses. These choices lead to the  $\xi$  dependent running coupling constant and running bottom quark mass,  $\alpha_s = 0.1411$  and  $m_b = 4.18$  GeV for the S-wave mass calcula-



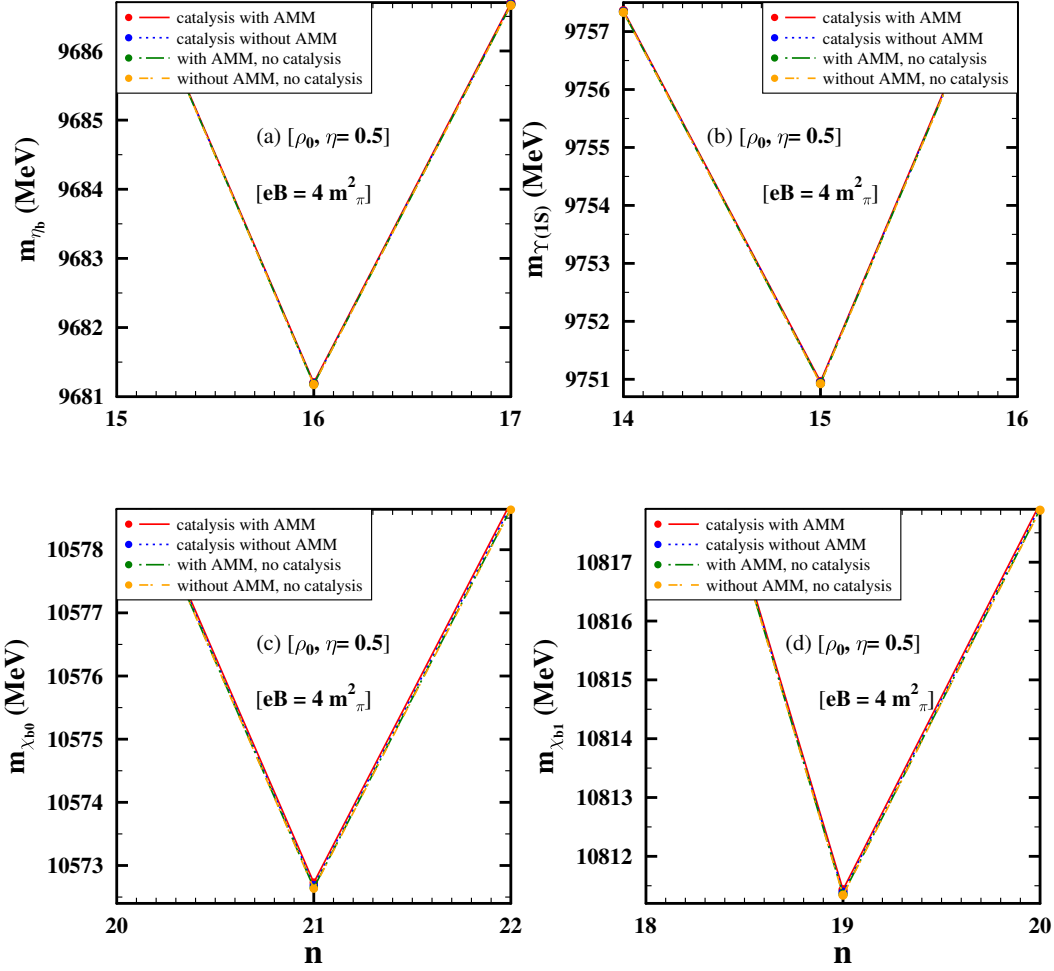


FIG. 14: Masses (MeV) are plotted as a function of  $n$ , for  $1S$  ( $\Upsilon(1S)$  and  $\eta_b$ ) and  $1P$  ( $\chi_{b0}$  and  $\chi_{b1}$ ) bottomonium states at  $\rho_B = \rho_0$  and  $\eta = 0.5$ . The effects of magnetized Dirac sea at  $eB = 4m_\pi^2$  are shown along with the case when only Landau level contributions of protons are taken into account. Plots are made with and without AMM effects of nucleons.

tions and  $\alpha_s = 0.1346$  and  $m_b = 4.13$  GeV for the P-wave mass calculations, respectively. With these parameters and with  $\phi_b$  calculated within the chiral effective model, the vacuum masses (in MeV) of  $\Upsilon(1S)$  and  $\eta_b$  are obtained to be 9751.24 and 9681.47 respectively. The vacuum masses (in MeV) of  $\chi_{b0}$  and  $\chi_{b1}$  are obtained as 10573.41 and 10812.1 respectively. The scalar fields are solved with and without the magnetized Dirac sea contributions at finite magnetic field along with the Landau level contribution of protons and the non zero

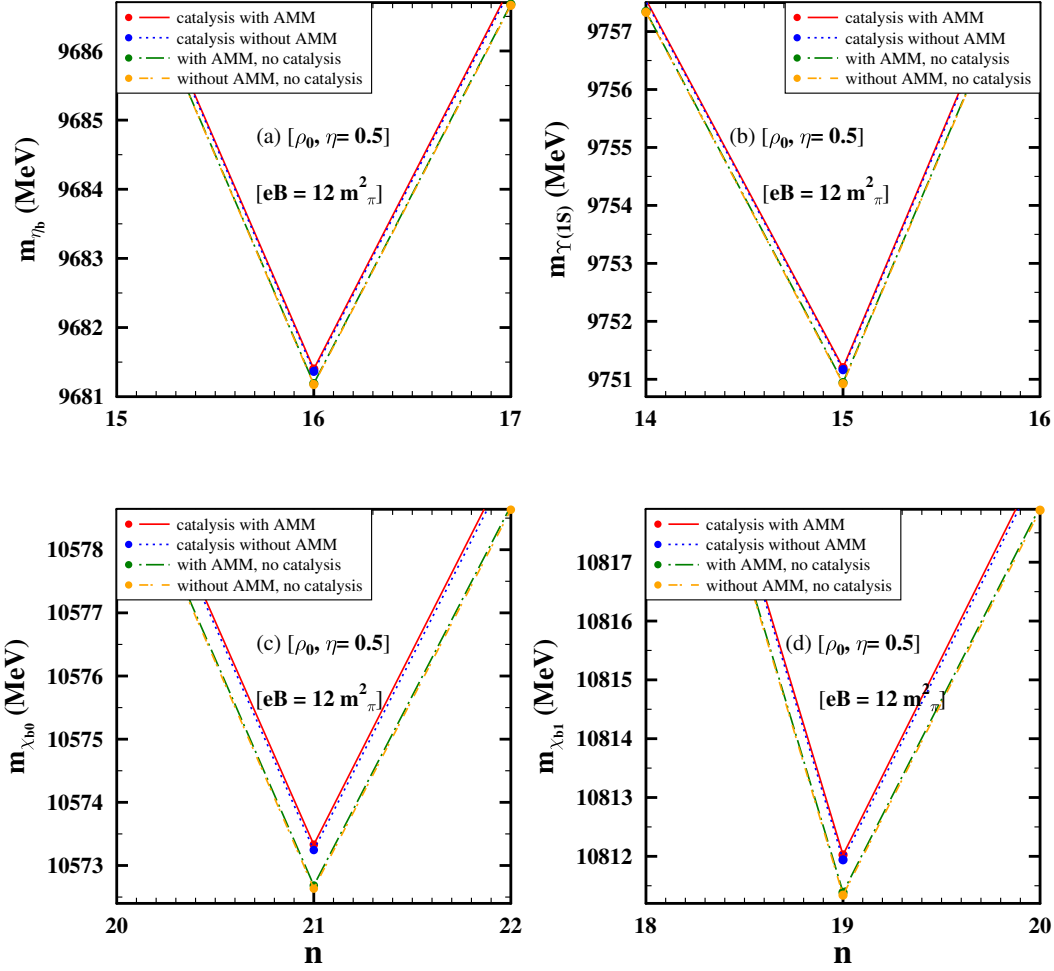


FIG. 15: Masses (MeV) are plotted as a function of  $n$ , for 1S ( $\Upsilon(1S)$  and  $\eta_b$ ) and 1P ( $\chi_{b0}$  and  $\chi_{b1}$ ) bottomonium states. The effects of magnetized Dirac sea on the masses, at  $eB = 12m_\pi^2$  are shown by comparing with the case when this effect is not considered over the Landau level contributions of protons. Plots are made with and without AMM effects of nucleons.

anomalous magnetic moments (AMM) of the nucleons at finite density. However, at zero density and finite magnetic field, there will be no contribution from the matter part through Landau quantization, but the vacuum polarizations of the nucleons give rise to some non trivial effects on the scalar fields.

The coupled equations of motion for the scalar fields are solved at zero density,  $\rho_B = 0$ , taking into account the magnetized vacuum polarizations of nucleons both for the zero and

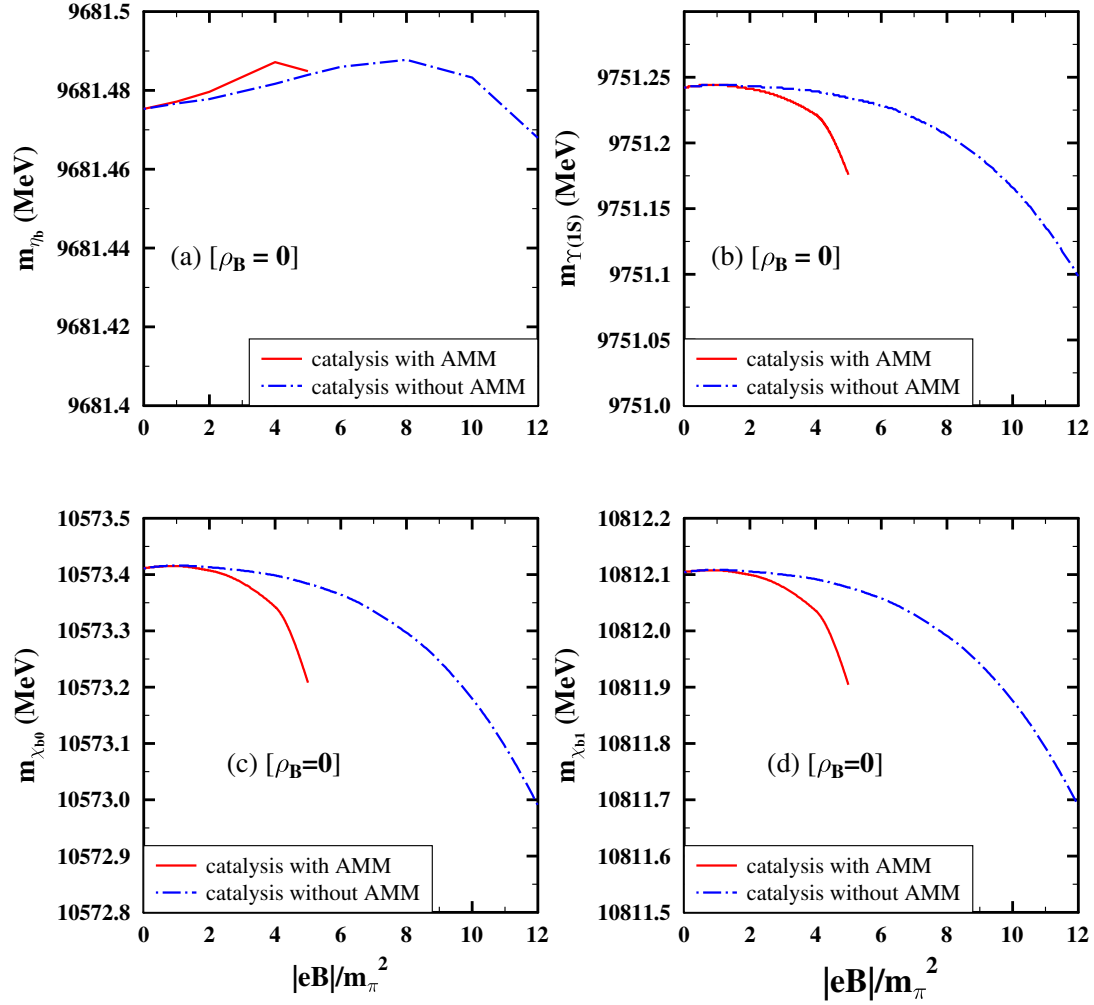


FIG. 16: Masses (MeV) are plotted as a function of  $|eB|$  (in units of  $m_\pi^2$ ) for 1S- ( $\Upsilon(1S)$  and  $\eta_b$ ) and 1P ( $\chi_{b0}$  and  $\chi_{b1}$ ) bottomonium states, at  $\rho_B = 0$ . At zero density, the variation in masses with magnetic field are only coming from the magnetized Dirac sea polarizations. There is no effect from Landau level quantization of protons or AMM effects of nucleons of the matter part at  $\rho_B = 0$ .

non-zero anomalous magnetic moments of the protons and neutrons. The values of the scalar fields associated to the QCD vacuum condensates, tend to rise with magnetic field, give rise to the effect called magnetic catalysis.

In-medium masses of the 1S and 1P bottomonia are thus computed within the sum rule approach by using the scalar and twist-2 gluon condensates in terms of the scalar fields

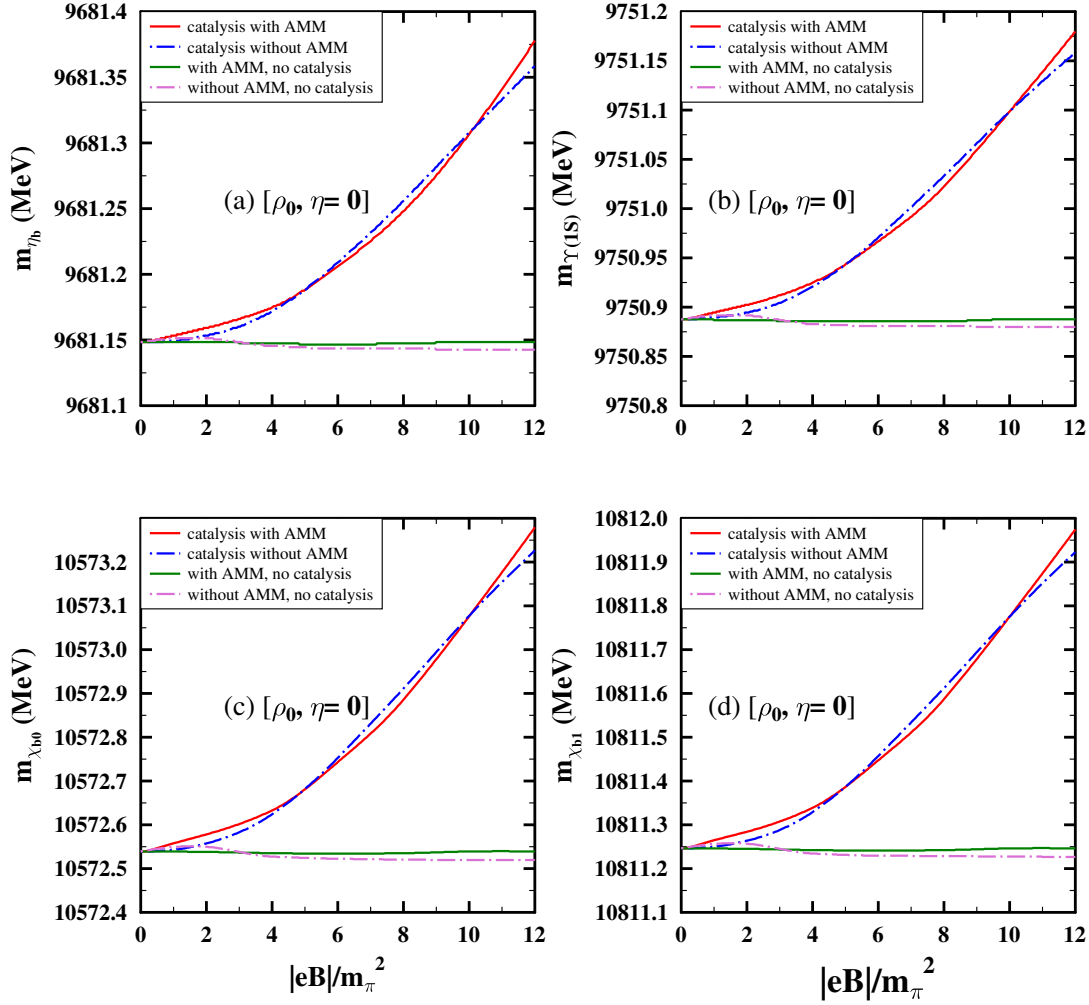


FIG. 17: Masses (MeV) are plotted as a function of  $|eB|$  (in units of  $m_\pi^2$ ) for 1S ( $Y(1S)$  and  $\eta_b$ ) and 1P ( $\chi_{b0}$  and  $\chi_{b1}$ ) bottomonium states at  $\rho_B = \rho_0$  and  $\eta = 0$ . The masses are computed incorporating the magnetized Dirac sea contribution, show the magnetic catalysis effect (solid line with AMM and dot-dashed line without AMM). Masses are compared to the case when only Landau level contributions of Fermi sea are considered (dotted line with AMM and long-dashed line for without AMM).

calculated in the chiral  $SU(3)$  model. In Fig.11, masses of all the four states are plotted as a function of the order of the moment,  $n$ . The value of  $n$  correspond to the minimum point gives the physical mass of the associated state. In this work, the masses plotted incorporating the effects of magnetized Dirac sea, are denoted as "catalysis with AMM" when the

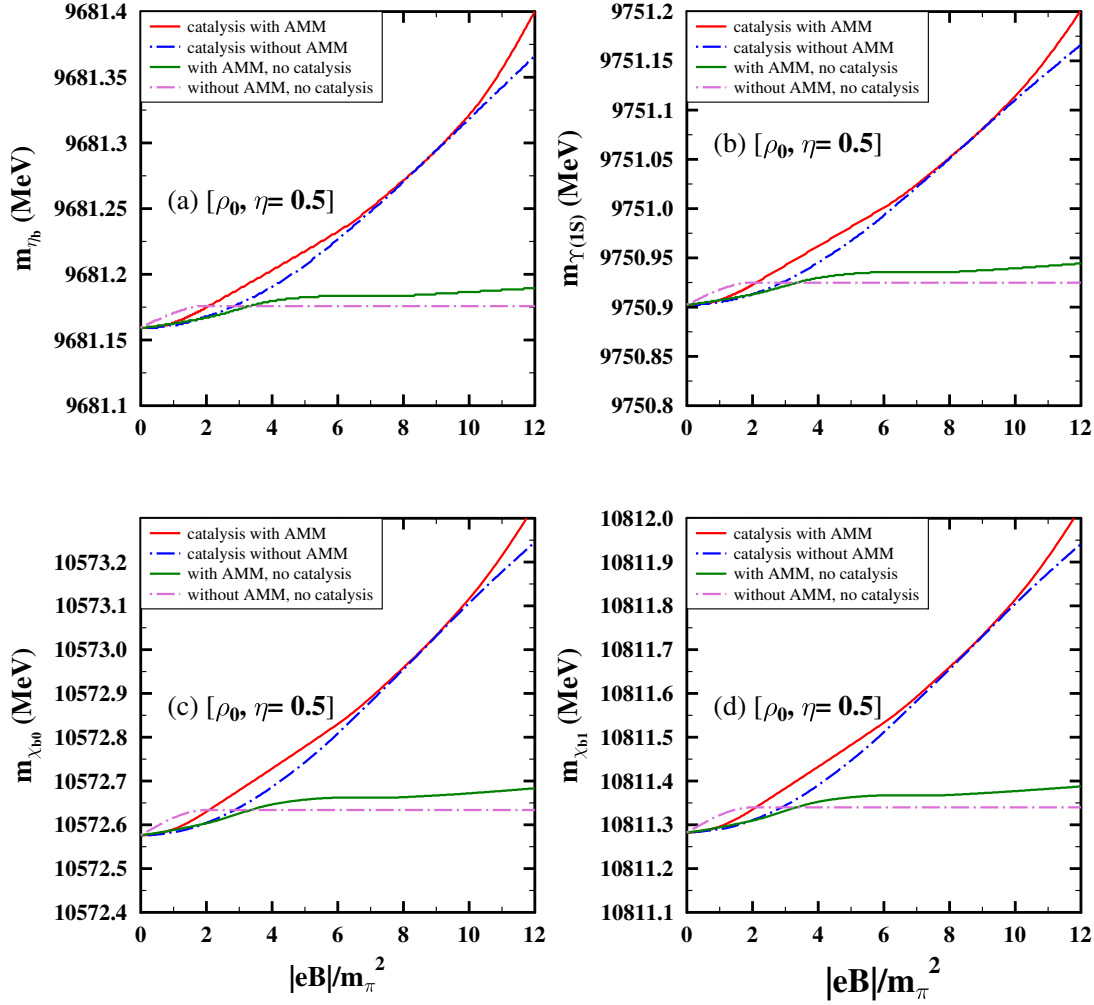


FIG. 18: Masses (MeV) are plotted as a function of  $|eB|$  (in units of  $m_\pi^2$ ) for 1S ( $Y(1S)$  and  $\eta_b$ ) and 1P ( $\chi_{b0}$  and  $\chi_{b1}$ ) bottomonium states at  $\rho_B = \rho_0$  and  $\eta = 0.5$ . The masses are computed incorporating the magnetized Dirac sea contribution, show the magnetic catalysis effect (solid line with AMM and dot-dashed line without AMM). Masses are compared to the case when only Landau level contributions of Fermi sea are considered (dotted line with AMM and long-dashed line for without AMM).

anomalous magnetic moments of the nucleons are considered and "catalysis without AMM" when not considered. In Figs.[12-15], the in-medium masses of the 1S-wave and 1P-wave states are plotted as a function of  $n$ , at nuclear matter saturation density,  $\rho_B = \rho_0$  for symmetric ( $\eta = 0$ ) as well as asymmetric ( $\eta = 0.5$ ) nuclear matter and at magnetic field values

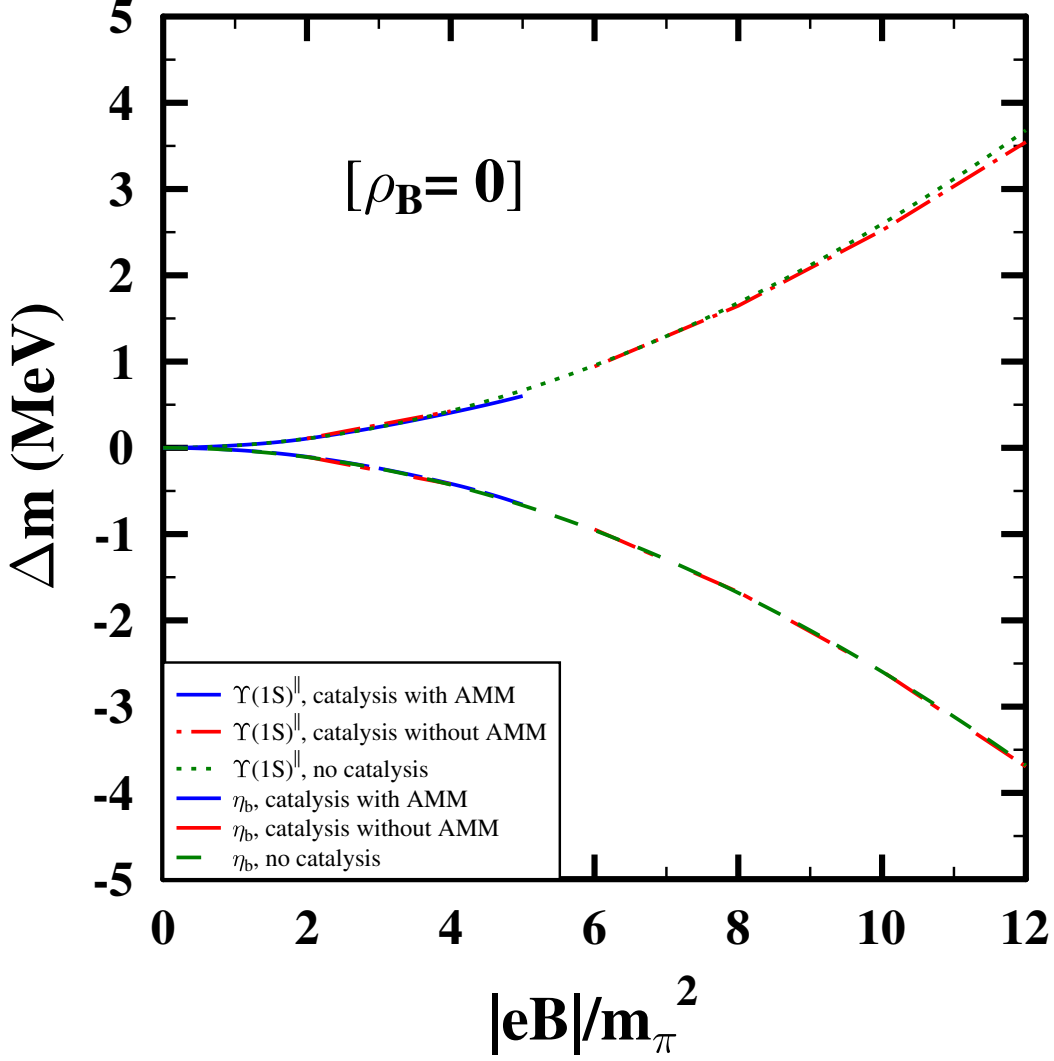


FIG. 19: Mass shifts (in MeV) are plotted as a function of  $|eB|$  (in units of  $m_\pi^2$ ) by considering the mixing between the longitudinal component of  $\Upsilon(1S)$  and  $\eta_b$ . Mixing effects are calculated with and without magnetized Dirac sea polarizations at  $\rho_B = 0$ .

of  $eB = 4, 12m_\pi^2$ . As can be seen from Fig.13 and Fig.15, the anomalous magnetic moments of the nucleons have distinguishable contribution on the masses in the case of catalysis effect as compared to the no catalysis case (when there is no Dirac sea contribution). In order to see the importance of the magnetic catalysis on the bottomonium masses, Figs.[17-18] illustrate the variation of mass with magnetic field and compare the two situations, when

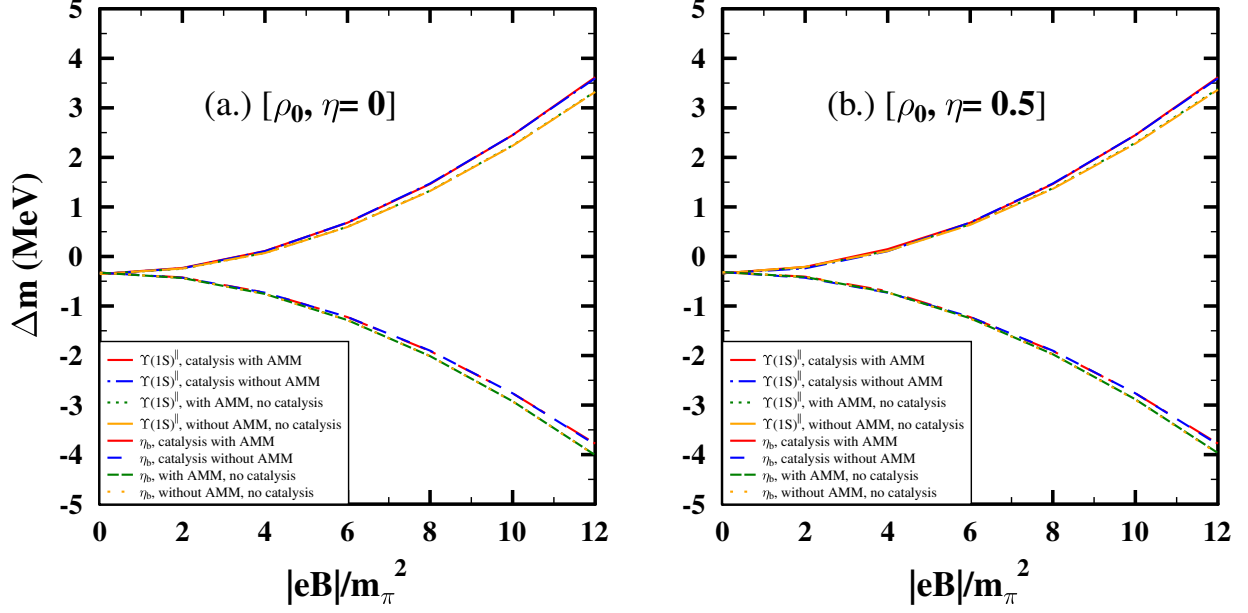


FIG. 20: Mass shifts (in MeV) are plotted as a function of  $|eB|$  (in units of  $m_\pi^2$ ) by considering the mixing between the longitudinal component of  $\Upsilon(1S)$  and  $\eta_b$ . Mixing effects are calculated with and without magnetized Dirac sea polarizations at  $\rho_B = \rho_0$ , in plot (a.) for symmetric nuclear matter ( $\eta = 0$ ) and plot (b.) for asymmetric matter ( $\eta = 0.5$ ).

the magnetic field modified Dirac sea polarizations are taken into account along with the Fermi sea effects and when magnetic field contributions are only on the nucleon Fermi sea through protons Landau levels and non-zero AMMs of the nucleons. The masses of the four lowest states of bottomonia increase with magnetic field at  $\rho_B = \rho_0$  and  $\eta = 0, 0.5$  for the case of magnetic catalysis. But there is no significant variation in the masses without catalysis effect. In Fig.16, the mass variation with magnetic field are shown for zero density,  $\rho_B = 0$ , and the behavior shown for  $\Upsilon(1S)$ ,  $\chi_{b0}$  and  $\chi_{b0}$  indicate a lowering of their masses with magnetic field whereas that of  $\eta_b$  is seen to rise at first up to  $eB = 8m_\pi^2$  (without AMM) then decrease. The masses are plotted up to  $eB = 5m_\pi^2$  at  $\rho_B = 0$  when including the anomalous magnetic moments of the nucleons. Thus, the effect of anomalous magnetic

moment on the bottomonium states are observed to be quite significant at zero density, and in presence of magnetized Dirac sea contribution. The different behavior of the pseudoscalar meson mass with magnetic field in the absence of nuclear matter, can be attributed to the variation in the Wilson coefficients for different channels.

The effect of the spin-magnetic field interaction on the longitudinal component of the vector meson,  $\Upsilon(1S)$  and the pseudoscalar meson,  $\eta_b$  is also studied here, using a Hamiltonian approach. The mass of the bottom quark is taken to be  $m_b = 4.7$  GeV in the expression for bottom quark Bohr magneton,  $\mu_b = \frac{e/3}{2m_b}$  to calculate the in-medium masses of  $\Upsilon^{\parallel}(1S)$  and  $\eta_b$  incorporating the spin-mixing effect. This effect give rise to increasing (decreasing) mass of the  $\Upsilon^{\parallel}(1S)$  ( $\eta_b$ ) with magnetic field. In Figs.[19-20] mass shifts of the  $\Upsilon^{\parallel}(1S)$  and  $\eta_b$  are plotted as a function of  $eB$  at  $\rho_B = 0$  and  $\rho_B = \rho_0$  for  $\eta = 0, 0.5$  both with and without catalysis effect.

## V. SUMMARY

To summarize the findings of the present work, the in-medium masses of both the S and P states of the heavy quarkonium (charmonium and bottomonium) states, calculated using a QCD sum rule approach, are observed to rise with magnetic field at the nuclear matter saturation density (both in symmetric as well as asymmetric nuclear matter), due to the magnetic catalysis effect arising from the magnetized Dirac sea polarization. At zero density, the effect of anomalous magnetic moment on the quarkonia masses are seen to be important through the magnetized Dirac sea contribution. The magnetic field has significant contribution on the masses of the quarkonia when taken through the Dirac sea effect in comparison to the no sea approximation. The magnetic field has dominant contribution on the 1S wave states through the vector-pseudoscalar mixing between the longitudinal component of the 1S spin triplet and 1S spin singlet states, which leads to an appreciable increase (decrease) in the masses of the  $J/\Psi^{\parallel}$  ( $\eta_c$ ) and  $\Upsilon^{\parallel}(1S)$  ( $\eta_b$ ). This might be observed as a quasi-peak at  $m_{\eta_c}$  and  $m_{\eta_b}$  in the dilepton spectra, as well as, can affect the  $J/\psi$  and  $\Upsilon(1S)$  production, in non-central ultra-relativistic collisions at RHIC, LHC, where the



magnetic fields produced are huge.

---

- [1] A. Hosaka, T. Hyodo, K. Sudoh, Y. Yamaguchi, S. Yasui, *Prog. Part. Nucl. Phys.* **96**, 88 (2017).
- [2] D. Kharzeev, L. McLerran and H. Warringa, *Nucl. Phys. A* **803**, 227 (2008).
- [3] K. Fukushima, D. E. Kharzeev and H. J. Warringa, *Phys. Rev. D* **78**, 074033 (2008).
- [4] V. Skokov, A. Y. Illarionov and V. Toneev, *Int. J. Mod. Phys. A* **24**, 5925 (2009).
- [5] W. T. Deng and X.G.Huang, *Phys.Rev. C* **85**, 044907 (2012).
- [6] K. Tuchin, *Adv. High Energy Phys.* **2013**, 490495 (2013).
- [7] E. Eichten, K. Gottfried, T. Kinoshita, K. D. Lane, and T. M. Yan, *Phys. Rev. D* **17**, 3090 (1978).
- [8] E. Eichten, K. Gottfried, T. Kinoshita, K. D. Lane, and T. M. Yan, *Phys. Rev. D* **21**, 203 (1980).
- [9] S. F. Radford and W. W. Repko, *Phys. Rev. D* **75**, 074031 (2007).
- [10] Frank Klingl, Sungsik Kim, Su Hounng Lee, Philippe Morath, and Wolfram Weise, *Phys. Rev. Lett.* **82**, 3396 (1999).
- [11] Sugsik Kim, Su Hounng Lee, *Nucl. Phys. A* **679**, 517 (2001).
- [12] Su Hounng Lee and Che Ming Ko, *Phys. Rev. C* **67**, 038202 (2003).
- [13] Arvind Kumar and Amruta Mishra, *Phys. Rev. C* **82**, 045207 (2010).
- [14] Amruta Mishra, Pallabi Parui, Ankit Kumar, and Sourodeep De, arXiv : 1811.04622 (nucl-th).
- [15] Pallabi Parui, Sourodeep De, Ankit Kumar, and Amruta Mishra, arXiv:2104.05471v1 [hep-ph] (2021).
- [16] R. Molina, D. Gamermann, E. Oset, and L. Tolos, *Eur. Phys. J A* **42**, 31 (2009); L. Tolos, R. Molina, D. Gamermann, and E. Oset, *Nucl. Phys. A* **827**, 249c (2009).
- [17] G. Krein, A. W. Thomas and K. Tsushima, *Prog. Part. Nucl. Phys.* **100**, 161 (2018).
- [18] G. Krein, A. W. Thomas and K. Tsushima, *Phys. Lett. B* **697**, 136 (2011).
- [19] Amal Jahan C.S., Shivam Kesarwani, Sushruth Reddy P., Nikhil Dhale, and Amruta Mishra, arXiv:1807.07572 (nucl-th).
- [20] Amal Jahan CS, Nikhil Dhale, Sushruth Reddy P, Shivam Kesarwani, Amruta Mishra, *Phys. Rev. C* **98**, 065202 (2018).

- [21] D. Kharzeev, K. Landsteiner, A. Schmitt, and H.-U. Yee, *Lect. Notes Phys.* **871**, 1 (2013).
- [22] M. D’Elia, S. Mukherjee, and F. Sanfilippo, *Phys. Rev. D* **82**, 051501 (2010).
- [23] D. Kharzeev, *Ann. Phys. (N.Y.)* **325**, 205 (2010); K. Fukushima, M. Ruggieri, and R. Gatto, *Phys. Rev. D* **81**, 114031 (2010).
- [24] A. J. Mizher, M.N. Chenodub, and E. Fraga, *Phys. Rev. D* **82**, 105016 (2010).
- [25] F. Preis, A. Rebhan, and A. Schmitt, *Lect. Notes Phys.* **871**, 51 (2013).
- [26] D. P. Menezes, M. Benghi Pinto, S. S. Avancini, and C. Providencia, *Phys. Rev. C* **80**, 065805 (2009); D.P. Menezes, M. Benghi Pinto, S. S. Avancini, A. P. Martinez, and C. Providencia, *Phys. Rev. C* **79**, 035807 (2009).
- [27] Bhaswar Chatterjee, Hiranmaya Mishra, and Amruta Mishra, *Phys. Rev. D* **84**, 014016 (2011).
- [28] Alexander Haber, Florian Preis, and Andreas Schmitt, *Phys. Rev. D* **90**, 125036 (2014).
- [29] Arghya Mukherjee, Snigdha Ghosh, Mahatsab Mandal, Sourav Sarkar, and Pradip Roy, *Phys. Rev. D* **98**, 056024 (2018).
- [30] G. S. Bali, F. Bruckmann, G. Endrodi, F. Gruber, and A. Schaefer, *J. High Energy Phys.* 04 (2013) 130.
- [31] Amruta Mishra and Divakar Pathak, *Phys. Rev. C* **90**, 025201 (2014).
- [32] Amruta Mishra, S.P. Misra, *Phys. Rev. C* **102**, 045204 (2020).
- [33] Amruta Mishra, S.P.Misra, *Phys. Rev. C* **95**, 065206 (2017).
- [34] S. Cho, K. Hattori, S. H. Lee, K. Morita and S. Ozaki, *Phys. Rev. D* **91**, 045025 (2015).
- [35] J. Schechter, *Phys. Rev. D* **21**, 3393 (1980).
- [36] Arata Hayashigaki , *Phys. Lett. B* **487**, 96 (2000); T. Hilger, R. Thomas and B. Kämpfer, *Phys. Rev. C* **79**, 025202 (2009); T. Hilger, B. Kämpfer and S. Leupold, *Phys. Rev. C* **84**, 045202 (2011); S. Zschocke, T. Hilger and B. Kämpfer, *Eur. Phys. J. A* **47** 151 (2011).
- [37] Z-G. Wang and Tao Huang, *Phys. Rev. C* **84**, 048201 (2011); Z-G. Wang, *Phys. Rev. C* **92**, 065205 (2015).
- [38] P. Gubler, K. Hattori, S. H. Lee, M. Oka, S. Ozaki and K. Suzuki, *Phys. Rev. D* **93**, 054026 (2016).
- [39] Amruta Mishra and S. P. Misra, *Int. J. Mod. Phys.E* **30** (2021) 08, 2150064.
- [40] Divakar Pathak and Amruta Mishra, *Int. J. Mod. Phy. E* **23**, 1450073 (2014).
- [41] Divakar Pathak and Amruta Mishra, *Phys. Rev. C* **91**, 045206 (2015).
- [42] Sushruth Reddy P, Amal Jahan CS, Nikhil Dhale, Amruta Mishra, J. Schaffner-Bielich, *Phys.*

- Rev. C **97**, 065208 (2018).
- [43] Nikhil Dhale, Sushruth Reddy P, Amal Jahan CS, Amruta Mishra, Phys. Rev. C **98**, 015202 (2018).
- [44] T. Hatsuda, S.H. Lee, Phys. Rev. C **46**, R34, (1992).
- [45] Amruta Mishra, Phys. Rev. C **91** 035201 (2015).
- [46] Amruta Mishra, Ankit Kumar, Pallabi Parui, Sourodeep De, Phys. Rev. C **100**, 015207 (2019).
- [47] Amruta Mishra, S.P. Misra, Int.J.Mod.Phys.E **31** (2022) 06, 2250060.
- [48] Amruta Mishra, S.P. Misra, arXiv: 1901.06259 (nucl-th).
- [49] A. Mishra, A. Jahan CS, S. Kesarwani, H. Raval, S. Kumar, and J. Meena, Eur. Phys. J. A **55** 99 (2019).
- [50] C. S. Machado, F. S. Navarra. E. G. de Oliveira and J. Noronha, Phys. Rev. D **88**, 034009 (2013).
- [51] C. S. Machado, R.D. Matheus, S.I. Finazzo and J. Noronha, Phys. Rev. D **89**, 074027 (2014).
- [52] K. Suzuki and S. H. Lee, Phys. Rev. C **96**, 035203 (2017).
- [53] Amruta Mishra, Anuj Kumar Singh, Neeraj Singh Rawat, and Pratik Aman, Eur.Phys.J.A **55** 107 (2019).
- [54] Amruta Mishra and S. P. Misra,, Int.J.Mod.Phys.E **30** (2021) 03, 2150014.
- [55] P. Papazoglou, D. Zschesche, S. Schramm, J. Schaffner-Bielich, H. Stöcker, and W. Greiner, Phys. Rev. C **59**, 411 (1999).
- [56] S.Weinberg, Phys. Rev. **166** 1568 (1968).
- [57] S. Coleman, J. Wess, B. Zumino, Phys. Rev. **177** 2239 (1969); C.G. Callan, S. Coleman, J. Wess, B. Zumino, Phys. Rev. **177** 2247 (1969).
- [58] W. A. Bardeen and B. W. Lee, Phys. Rev. **177** 2389 (1969).
- [59] A. Mishra, K. Balazs, D. Zschesche, S. Schramm, H. Stöcker, and W. Greiner, Phys. Rev. C **69**, 024903 (2004).
- [60] D. Zschesche, A. Mishra, S. Schramm, H. Stöcker and W. Greiner, Phys. Rev. C **70**, 045202 (2004).
- [61] Erik K. Heide, Serge Rudaz and Paul J. Ellis, Nucl. Phys. A **571**, (2001) 713.
- [62] A. Broderick, M. Prakash and J.M.Lattimer, Astrophys. J. **537**, 351 (2002).
- [63] A.E. Broderick, M. Prakash and J. M. Lattimer, Phys. Lett. B **531**, 167 (2002).
- [64] F. X. Wei, G. J. Mao, C. M. Ko, L. S. Kisslinger, H. Stöcker, and W. Greiner, J. Phys. G,

- Nucl. Part. Phys. **32**, 47 (2006).
- [65] Guang-Jun Mao, Akira Iwamoto, Zhu-Xia Li, Chin. J. Astrophys. **3**, 359 (2003).
- [66] M. Pitschmann and A. N. Ivanov, arXive : 1205.5501 (math-ph).
- [67] V. Dexheimer, R. Negreiros, S. Schramm, Eur. Phys. Journal A **48**, 189 (2012).
- [68] V. Dexheimer, B. Franzon and S. Schramm, Jour. Phys. Conf. Ser. **861**, 012012 (2017).
- [69] R. M. Aguirre and A. L. De Paoli, Eur. Phys. J. A **52**, 343 (2016).
- [70] K. Morita and S.H. Lee, Phys. Rev. Lett **100**, 022301 (2008); K. Morita and S.H. Lee, Phys. Rev. C **77**, 064904 (2008); S.H. Lee and K. Morita, Phys. Rev. D **79**, 011501(R) (2009); S.H. Lee and K. Morita, Pramana Journal of Physics **72**, 97 (2009); K. Morita and S.H. Lee, Phys. Rev. C **85**, 044917 (2012).
- [71] Thomas D. Cohen, R. J. Furnstahl and David K. Griegel, Phys. Rev. C **45**, 1881 (1992).
- [72] L. J. Reinders, H. R. Rubinstein, and S. Yazaki, Nucl. Phys. B **186**, 109 (1981).
- [73] L. J. Reinders, H. R. Rubinstein, and S. Yazaki, Physics reports **127**, 1 (1985).
- [74] Young-Ho Song, S.H. Lee, K. Morita, Phys. Rev. C **79**, 014907 (2009).
- [75] S. Cho, K. Hattori, S. H. Lee, K. Morita and S. Ozaki, Phys. Rev. Lett. **113**, 122301 (2014).
- [76] J. Alford and M. Strickland, Phys. Rev. D **88**, 105017 (2013).
- [77] K. Suzuki and S. H. Lee, Phys. Rev. C **96**, 035203 (2017).
- [78] P.A. Zyla et al. (Particle Data Group), Prog. Theor. Exp. Phys. **2020**, 083C01 (2020).